ChemComm

FEATURE ARTICLE

View Article Online
View Journal | View Issue

Cite this: *Chem. Commun.*, 2014, **50**, 10355

Received 5th April 2014,
Accepted 2nd June 2014

DOI: 10.1039/c4cc02515f

www.rsc.org/chemcomm

Key processes in ruthenium-catalysed olefin metathesis

David J. Nelson,† Simone Manzini, César A. Urbina-Blanco‡ and Steven P. Nolan*

While the fundamental series of [2+2]cycloadditions and retro[2+2]cycloadditions that make up the pathways of ruthenium-catalysed metathesis reactions is well-established, the exploration of mechanistic aspects of alkene metathesis continues. In this Feature Article, modern mechanistic studies of the alkene metathesis reaction, catalysed by well-defined ruthenium complexes, are discussed. Broadly, these concern the processes of pre-catalyst initiation, propagation and decomposition, which all have a considerable impact on the overall efficiency of metathesis reactions.

Introduction

The metathesis reaction catalysed by well-defined homogeneous transition metal complexes has become a staple technique for the synthesis of a number of molecules. This progress was recognised in 2005 with the award of the Nobel Prize in Chemistry to Yves Chauvin, Robert Grubbs and Richard Schrock, for their work in this area.[1–3] Metathesis reactions proceed *via* carbene exchange between a metal carbene and an alkene (Scheme 1(a)); a metallacyclobutane (MCB) is the intermediate species. Astruc and Lloyd-Jones have discussed early work on elucidating this basic mechanism.[4,5] This basic series of steps can be used to design a variety of processes, such as: ring-closing metathesis (RCM) in which a diene substrate forms a cycloalkene plus an alkene; cross-metathesis (CM) in which two alkenes are used to prepare two new alkenes; ring-opening metathesis polymerisation (ROMP) where a cyclic alkene is used to prepare a polymer; and acyclic diene metathesis (ADMET) where a diene substrate is polymerised to form a poly(alkene) chain (Scheme 1(b)). A wide range of pre-catalysts are known, the majority of which bear N-heterocyclic carbene (NHC) ligands,[6–8] although the basic mechanism is the same in each case.[9] Metathesis pre-catalysts are known that bear various ancillary ligands, alkylidenes, and halides (*e.g.* Fig. 1).[6,7,10–19] Metathesis pre-catalysts typically feature a so-called "throw-away" ligand which is not present in the active catalyst; this is typically a chelating alkoxystyrene group or a phosphine, although a wide range of such ligands have been employed.

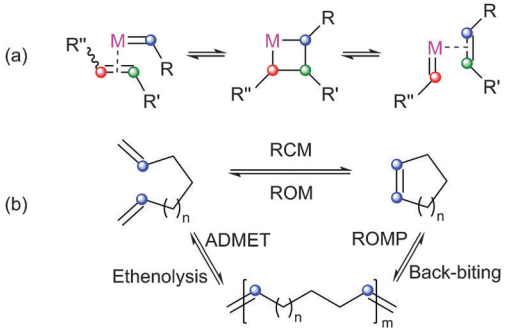

Scheme 1 (a) The general [2+2] cycloaddition mechanism; (b) examples of metathesis transformations.

Work continues in this field, to elucidate the finer mechanistic details. Here, we consider the developments that are of most relevance to the ruthenium-catalysed homogeneous alkene metathesis reaction, for which a more detailed mechanistic outline can be found in Scheme 2. Key processes include: the study of pre-catalyst initiation, during which a stable pre-catalyst (typically 16e$^-$ Ru^{II}) becomes an active 14e$^-$ species; the study of how the ancillary ligand affects reactivity; the partitioning between intra- and inter-molecular metathesis pathways; the study and understanding of the key steps that occur during metathesis reactions, the development of *Z*-selective metathesis pre-catalysts; and the study of catalyst decomposition. Tandem catalysis (involving a metathesis step and a subsequent reaction using the same charge of ruthenium) and deleterious side reactions such as unwanted isomerisation are beyond the scope of this Review and are mentioned only briefly. While experimental studies are the main focus, a selected number of salient examples of computational studies will be discussed. Aspects of the latter topic were reviewed recently by Cavallo *et al.*[20] and by van Sittert *et al.*[21]

EaStCHEM School of Chemistry, University of St Andrews, North Haugh, St Andrews, Fife, KY16 9ST, UK. E-mail: snolan@st-andrews.ac.uk

† Current address: WestCHEM Department of Pure and Applied Chemistry, University of Strathclyde, 295 Cathedral Street, Glasgow, G1 1XL, UK.

‡ Current address: Lehrstuhl für Technische Chemie und Petrolchemie, Institut für Technische und Makromolekulare Chemie (ITMC), RWTH Aachen University, Worringerweg 1, 52074 Aachen, Germany.

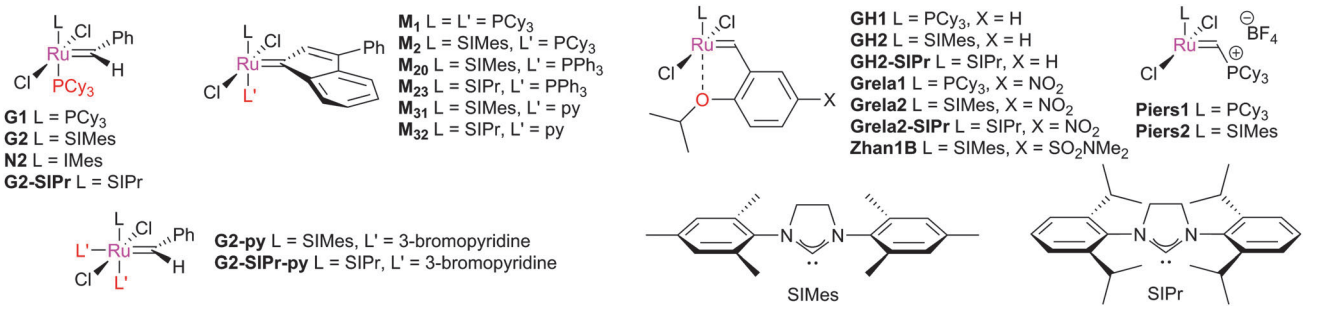

Fig. 1 Common metathesis pre-catalysts; **G** indicates Grubbs-type; **N**, Nolan, **M**, Unmicore 'M' series indenylidene complexes; **GH2**, Grubbs–Hoveyda type.

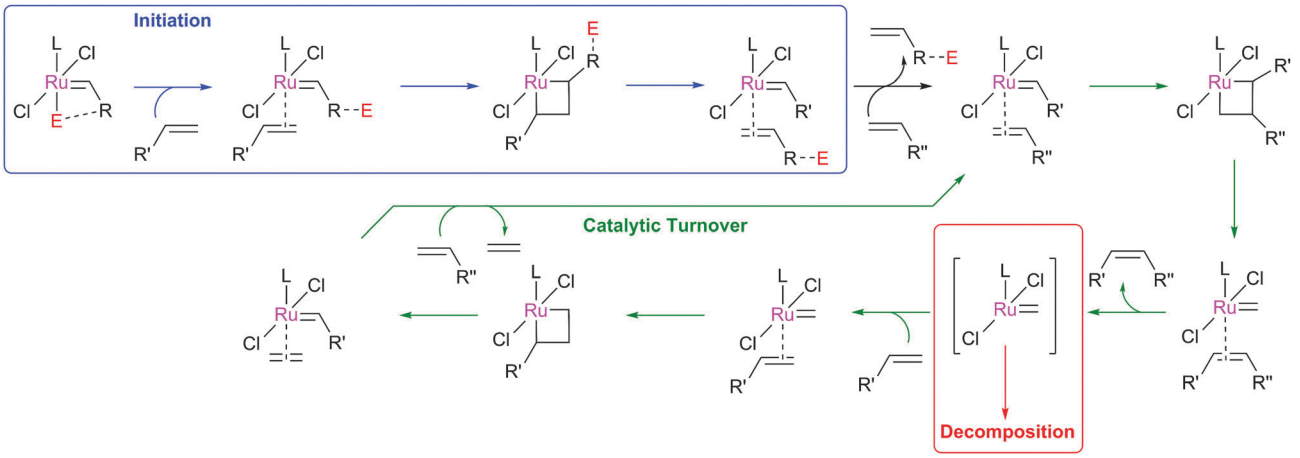

Scheme 2 Key stages of alkene metathesis reactions.

Pre-catalyst initiation

The initiation rate of a pre-catalyst determines the rate at which active $14e^-$ species are generated; this factor has a significant impact on the overall reaction. Most pre-catalysts are $16e^-$ species which must first lose a ligand to generate a (typically unobservable) $14e^-$ alkylidene. This process has been studied heavily, particularly in recent years. Notably, the use of well-defined catalysts rather than ill-defined salts or heterogeneous catalysts has allowed the key steps during initiation to be studied in some detail. Initiation mechanisms are considered here for several selected pre-catalyst types; for $16e^-$ pre-catalysts the initiation can be considered to be one of three types: associative, dissociative, or interchange (Scheme 3). In the former, alkene binds the metal centre to yield an $18e^-$ intermediate before loss of a ligand; in the dissociative mechanism, a $14e^-$ species is first formed that binds alkene; and in the interchange mechanism the binding of alkene and loss of a ligand occur simultaneously.

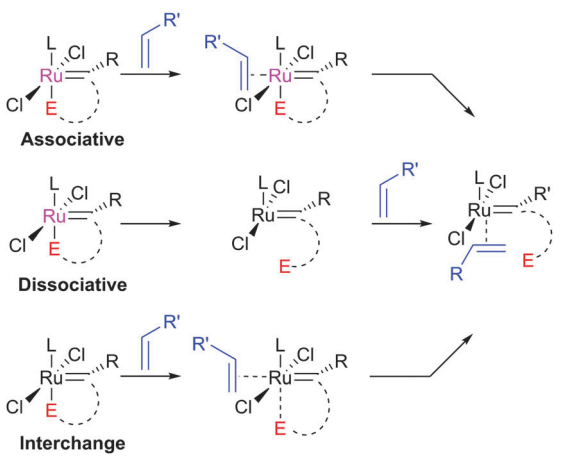

Scheme 3 Three mechanisms for pre-catalyst activation.

Phosphine-containing pre-catalysts (Grubbs-type)

Initially, the metathesis reaction catalysed by **G1** was believed to occur *via* an associative mechanism, *via* an intermediate such as **1**.[22] Phosphine dissociation was proposed to then allow MCB formation subsequently. Highly σ-donating phosphines were proposed to be best able to stabilise the MCB. Later work established that the first step in the mechanism was in fact phosphine dissociation (*i.e.* a dissociative process).[23]

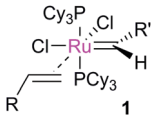

1

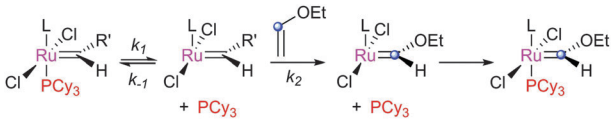

Scheme 4 Initiation rate measurements *via* reaction with ethyl vinyl ether.

Two methods were used to probe this process: (i) ^{31}P NMR spectroscopy, to probe the rate of exchange of free phosphine with bound phosphine, and (ii) the reaction of the pre-catalysts with ethyl vinyl ether (EVE), for which phosphine dissociation was shown to be rate limiting (Scheme 4). Interestingly, **G2** initiated much slower than **G1**, despite the much greater σ-donating ability of SIMes *versus* PCy_3.[24] Instead, the origin of the higher rate of activity of second generation complexes was found to be due to the preference of second generation alkylidenes for alkene over phosphine (*vide infra*). Initiation rates have been collected for a range of phosphine-bearing benzylidene complexes, with less electron-donating phosphines dissociating more readily.[25,26] Initiation rates for **G2** are known in a number of solvents,[27] including some fluorinated aromatic solvents that have been proposed to enhance reactivity.[28,29] Notably, changes to the dissociating phosphine ligand do not change the nature of the active species; the same 14e$^-$ alkylidene is generated upon initiation.

The differences in initiation between first- and second-generation pre-catalysts have intrigued many chemists. Initially, it was thought that the higher *trans*-effect of the NHC *versus* the phosphine should render the activation of **G2** faster than that of **G1**. However, Kennepohl has shown, using Ru K-edge X-ray absorption spectroscopy, that the metal centre of **G2** is in fact more electron deficient than in **G1** due to d to π* back-bonding in **G2**.[30] DFT studies have sought to reproduce the experimental initiation data. Some key studies deserve special mention: Truhlar has shown the importance of dispersive interactions in calculating initiation rates;[31] Goddard has successfully reproduced experimental energies, but required the use of an explicit solvent molecule to occupy the vacant site on the product 14e alkylidene;[32] Jensen has carried out detailed calculations for a number of complexes, achieving good agreement with experiment using counterpoise- and dispersion-corrected B3LYP calculations;[33] and Truhlar has also proposed that carbene rotamer switching is the underlying cause of the intriguing initiation rate differences between **G1** and **G2**.[34]

Nolan has studied the initiation of indenylidene species such as $\mathbf{M_{20}}$ and $\mathbf{M_{23}}$, using [^{31}P, ^{31}P] EXSY and EVE quench experiments.[35] The indenylidene moiety was shown to lead to a decrease in initiation rate compared to the analogous benzylidene complexes. However, most interestingly, $\mathbf{M_{20}}$ was shown to initiate *via* an interchange mechanism rather than a dissociative mechanism; *i.e.* alkene binding and phosphine dissociation occur during one concerted step. Activation parameters showed a negative entropy of activation ($\Delta S^{\ddagger} = -13 \pm 8$ cal K^{-1} mol^{-1}) for $\mathbf{M_{20}}$ *versus* a positive entropy of activation for complexes such as $\mathbf{M_1}$ ($\Delta S^{\ddagger} = 8 \pm 4$ cal K^{-1} mol^{-1}), **G2** ($\Delta S^{\ddagger} = 12 \pm 10$ cal K^{-1} mol^{-1}), and $\mathbf{M_{23}}$ ($\Delta S^{\ddagger} = 21 \pm 3$ cal K^{-1} mol^{-1}). DFT calculations were performed to support this work, which indicated a rather fine balance between dissociative and interchange mechanisms, with typically only a few kcal mol^{-1} difference between the two pathways.

Table 1 Initiation rate constants and thermodynamic parameters for selected phosphine-containing pre-catalysts at 353 K

Complex	k_{init}	$\Delta H^{\ddagger}$ (kcal mol^{-1})	$\Delta S^{\ddagger}$ (cal K^{-1} mol^{-1})	$\Delta G^{\ddagger}$ (kcal mol^{-1})
G1	9.6(2) s^{-1}	23.6(5)	12(2)	19.88(6)
G2	0.13(1) s^{-1}	27(2)	13(6)	23.0(4)
$\mathbf{M_1}$	1.72 s^{-1}	23(1)	8(4)	21(2)
$\mathbf{M_{20}}$	0.19 L mol^{-1} s^{-1}	17(3)	−13(8)	21(4)

A table of activation rates for selected phosphine-containing pre-catalysts can be found in Table 1, illustrating how these span a considerable range.

Chelating benzylidene-ether pre-catalysts (Hoveyda-type)

Initially, Hoveyda-type complexes were proposed to initiate *via* a dissociative mechanism, where the transition state (TS) involves partial rotation of the alkylidene and scission of the Ru–O bond (Fig. 2).[26] Later work showed that the entropy of activation was actually negative[36] ($\Delta S^{\ddagger}$ for **GH2** = -19 ± 3 cal K^{-1} mol^{-1}), consistent with either an interchange mechanism, where Ru–O scission occurs in tandem with the approach of the alkene substrate, or the associative mechanism where a six-coordinate intermediate forms before Ru–O bond scission. The first detailed study of the initiation mechanism of this class of catalysts was carried out by Plenio, who studied the initiation of **GH2** and **Grela2** using UV/visible spectroscopy.[37] Kinetic experiments showed that the initiation rates of **GH2** and **Grela2** depended on the identity and concentration of the alkene substrate. Subsequently, Percy and Hillier studied the initiation of **GH2** using kinetic experiments and DFT calculations.[38] Experimental and theoretical activation parameters for this complex were in agreement. The dissociative, associative and interchange mechanisms were all studied *in silico*, with the latter presenting the lowest barrier.

Following this, Plenio and co-workers published a detailed study of a range of complexes and substrates.[39] A mixture of dissociative and interchange mechanisms was proposed to operate, with the balance of these processes dependent on the pre-catalyst and substrate. Much of this was based on the observed curvature of a plot of k_{obs} *versus* [substrate].

In a detailed computational study, Solans-Monfort and co-workers modelled the initiation of some Hoveyda-type complexes with model substrates.[40] Notably, they pointed out that the choice of starting point can affect the outcome: if a pre-reactant complex

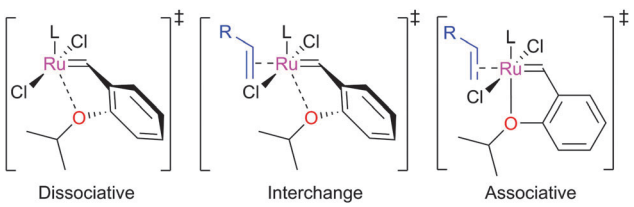

Fig. 2 Transition states for Hoveyda-type pre-catalyst initiation.

is considered, the entropic cost of associative/interchange mechanisms is underestimated; if not, it may be overestimated. The authors ruled out the associative mechanism, but could not firmly distinguish between the interchange and dissociative mechanisms. The final dissociation of the η^2-vinylaryl moiety was also proposed to have a large barrier, which may affect the overall rate.

Initiation rates for a number of Hoveyda-type complexes have been published.[39,41,42] The SIPr ligand significantly decreases the initiation rate of these complexes, in contrast to the trend observed with Grubbs-type species;[42] **GH2-SIPr** initiates *ca.* 10-fold slower than **GH2**. In addition, initiation rates for **GH2** have been recorded in a range of solvents.[27]

A later computational study by Hillier, Percy, and co-workers evaluated the potential energy surfaces (PES) for the initiation of three complexes with a selection of substrates.[43] The metathesis of ethene was found (both experimentally and computationally) to be energetically unfavourable overall, while the metathesis of EVE was highly favourable. Notably, the barriers on the PES for metallacyclobutanation are as high as those for the initial interchange step, suggesting that more than one step in the sequence has a considerable influence on the overall rate.

Naphthalene-based Hoveyda-type complexes have been explored in metathesis; studies of complexes **2–4** suggest that the degree of aromaticity is important in determining initiation rate.[44] Barbasiewicz *et al.* later synthesised the corresponding *peri*-substituted naphthyl-based complex **5**, which was shown to be a more rapid initiator than other naphthyl-based systems.[45]

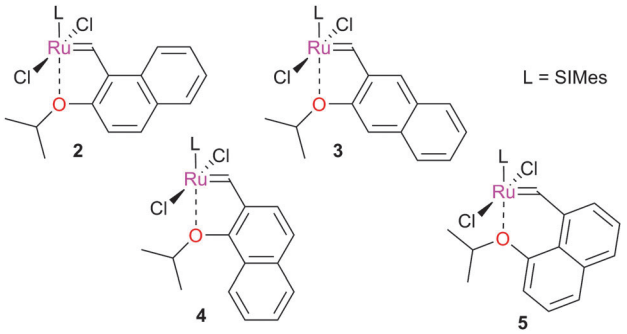

A table of activation rates for selected Hoveyda-type pre-catalysts can be found below (Table 2).[38,41–43] Electron-withdrawing or bulky substituents accelerate the initiation, compared to electron-donating groups.

Table 2 Initiation rate constants and thermodynamic parameters for selected Hoveyda-type pre-catalysts with ethyl vinyl ether at 298 K

Complex	k_{init} (L mol^{-1} s^{-1})	$\Delta H^{\ddagger}$ (kcal mol^{-1})	$\Delta S^{\ddagger}$ (cal K^{-1} mol^{-1})	$\Delta G^{\ddagger}$ (kcal mol^{-1})
GH2	0.02642	14.1(1.2)	−18.5(5.0)	19.6(2.0)
Grela2	0.3172	12.4(1.0)	−19.3(3.5)	18.2(1.7)
Zhan1B	0.1320	—[a]	—[a]	—[a]
GH2-SIPr	2.956×10^{-3}	—[a]	—[a]	—[a]
Grela2-SIPr	0.03675	—[a]	—[a]	—[a]

[a] Not determined.

Vinylphosphonium complexes (Piers-type)

These species[17] initiate rapidly, which has led to their use for interesting mechanistic studies that would be very difficult to accomplish otherwise.[46–53] The basic initiation mechanism involves a [2+2]cycloaddition with ethene, which releases a vinylphosphonium byproduct and generates the 14e$^-$ methylidene rapidly (Scheme 5).[49] The byproduct was shown to be a Type IV olefin[54] (*vide infra*) which does not undergo metathesis. Piers-type catalysts smoothly form Hoveyda-type complexes if exposed to the corresponding alkoxystyrene. Competing dimerisation can occur (*vide infra*), but this can be mitigated by the appropriate phosphonium substitution pattern, with triisopropylphosphine-based complexes highlighted as striking the best balance between stability and reactivity.

Phosphite complexes (Cazin-type)

Cazin and co-workers have recently prepared and studied a series of NHC–phosphite complexes. Phosphites are more π-acidic, and have different electronic and steric properties, compared to phosphines.[55] Cazin reported the synthesis of **Caz1** *via* simple ligand displacement (Scheme 6).[56,57]

Surprisingly, the product complex featured *cis*-chloride rather than the expected *trans*-chloride geometry. Analogous benzylidene complexes exhibit the expected *trans*-geometry.[58] For SIPr-bearing indenylidene species, the use of P(OEt)$_3$ leads to the *trans*-chloride complex, while for P(O^{i}Pr)$_3$ only the *cis*-species can be accessed.[59] **Caz-1** must undergo a *cis-trans* isomerisation before yielding an active 14e$^-$ species by ligand dissociation. The barrier is considerable ($\Delta H^{\ddagger}$ = 22.6 kcal mol^{-1}; $\Delta S^{\ddagger}$ = −4.2 cal K^{-1} mol^{-1}),[56] and so the catalyst is only active at high temperatures, but exhibits excellent stability under ambient conditions. The addition of excess phosphite did not affect the

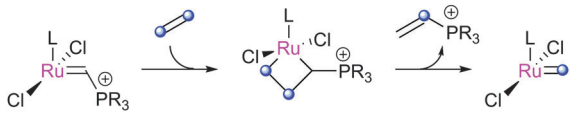

Scheme 5 Initiation of Piers-type complexes.

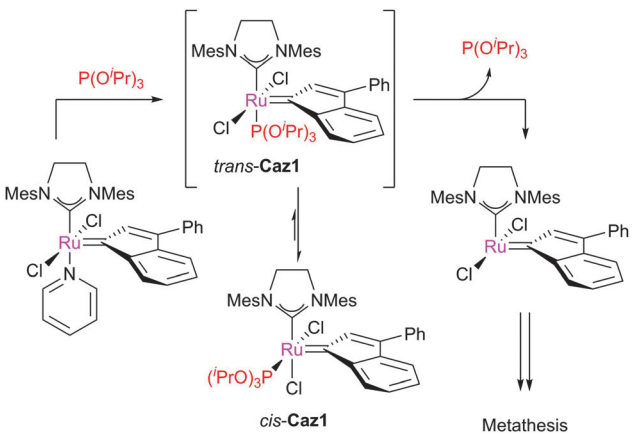

Scheme 6 Synthesis and initiation of Cazin-type pre-catalysts.

rate of isomerisation, suggesting that ligand dissociation/re-association was not involved.

Heteroatom-chelated complexes

Latent complexes, typically bearing chelating nitrogen- or sulfur-based functionality, have also attracted attention.[60,61] High stability and low activity under ambient conditions allow for easy handling, before activation using a specific stimulus such as light, heat, or an additive. Some studies have been conducted on the behaviour of some of these complexes, to investigate parameters relevant to their initiation, mainly around their *cis–trans* isomerisation. This issue is relevant to initiation, as these two isomers will exhibit different initiation behaviours.

Quinoline complexes such as **6** and **7** exist in either *cis*- or *trans*-geometries, which interconvert when heated (Scheme 7).[62] The *trans*-isomer is the most active in catalysis, although reactivity at room temperature was much poorer than common pre-catalysts such as **G2**. DFT studies suggested that the pathway in which the nitrogen remained bound to the ruthenium during this isomerisation was lowest in energy; however, there was a small difference between this pathway and the one in which the Ru–N bond is disrupted and re-formed.[63] Sulfur- and halide-chelated complexes also exhibit isomerisation from the *trans*- to the *cis*-configuration,[64,65] although such processes have not been studied in as much detail for these systems.[66] For some complexes, the intermediate *trans*-isomer is not observable.

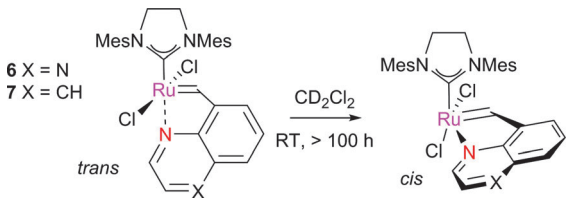

Scheme 7 Isomerisation of quinolone-based complexes.

Grela *et al.* studied the initiation of six co-ordinate complexes such as **8**;[67] these were found to be more reactive than the parent complexes (*e.g.* **9**). DFT studies revealed that this was the result of a different initiation mechanism, where the pyridine ligand assisted debinding of the sulfoxide and thus co-ordination of the alkene substrate.

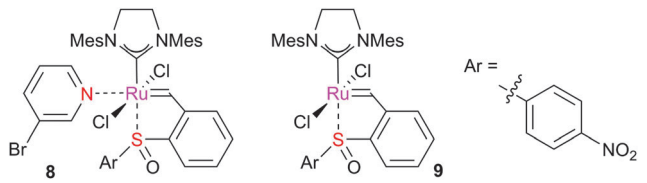

Pyridine-bearing complexes

The study of rapidly initiating pyridine-bearing complexes has been explored recently. Initially, only an estimate of initiation rate for species such as **G2-py** was available.[13] Trzaskowski and Grela recently investigated the initiation of complexes of this type using DFT calculations.[68] Three mechanisms were considered: one where the (bromo)pyridine ligands dissociate before alkene binding, one where alkene binding occurs with a (bromo)pyridine ligand attached (*via* an intermediate six coordinate complex), and one where the second (bromo)pyridine ligand is displaced by substrate in an interchange fashion. The authors concluded that the dissociative mechanism was favoured, although for small substrates the associative mechanism was plausible.

Metathesis propagation

While the initiation event is critical in determining how quickly 14e$^-$ active species are formed, the actions and activities of these species also determine the overall efficiency of the reaction.

First- *versus* second-generation pre-catalysts

Since the introduction of the first NHC-bearing complexes, significant differences in reactivity have been apparent between these second generation complexes and the bis(phosphine) first generation pre-catalysts. While early second generation species, such as Herrmann's bis(NHC) complexes[69] performed poorly, it was realised quickly that heteroleptic NHC–phosphine[12,19,70] and NHC–chelating ether[15] complexes showed better reactivity. As discussed above, this reactivity difference was despite the much slower initiation of second generation complexes, as discovered by Grubbs and co-workers,[23] who conducted a series of experiments to explore the differences between first- and second-generation metathesis complexes.[25] When these complexes were exposed to defined ratios of EVE and phosphine, reversible phosphine binding could compete with the (effectively irreversible)[71] reaction with EVE (Scheme 8). The observed pseudo-first order rate constants for the decrease of pre-catalyst concentration plotted *versus* [phosphine]/[EVE] furnished a straight line with intercept $1/k_{init}$ and gradient $k_{rebind}/(k_{init}\cdot k_{metathesis})$ (eqn (1); Fig. 3). **G2** is equally selective for phosphine and alkene, while **G1** is 10^3 times more selective for phosphine. While **G1** initiates more rapidly, it is less likely to undergo productive metathesis before being trapped by phosphine; the initiation rates alone do not determine the overall reactivity, as one must consider the activity and selectivity of the 14e$^-$ species also.

$$1/k_{obs} = (k_{rebind}\cdot[PCy_3])/(k_{init}\cdot k_{metathesis}\cdot[EVE]) + 1/k_{init} \qquad (1)$$

As well as this general difference in behaviour towards alkenes, first- and second-generation catalyst systems will react differently with some substitution patterns found in substrates. Grubbs *et al.* developed a useful system of classification for alkene termini, predominantly for use in predicting or rationalising CM reaction outcomes.[54] Each alkene structural motif can be categorised as Type I–IV. Type I alkenes react

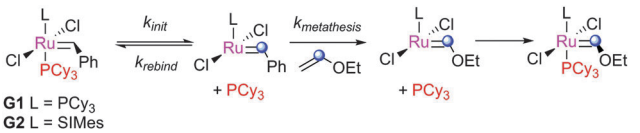

Scheme 8 Probing the selectivity of **G1** and **G2** for alkene *versus* phosphine.

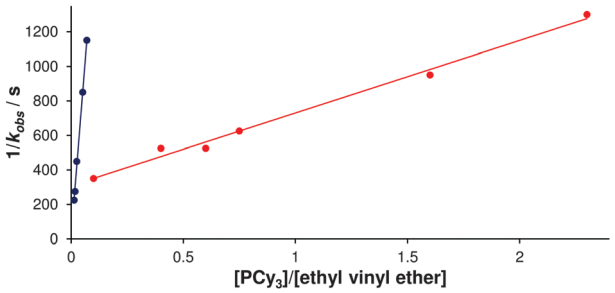

Fig. 3 Plot of $1/k_{obs}$ *versus* [PCy_3]/[ethyl vinyl ether] for the metathesis of EVE with **G1** (blue) and **G2** (red) in the presence of added PCy_3.[25]

(and dimerise) quickly, but dimers are consumable; a number of alkenes have been charged to CM reactions as the dimer. Type II alkenes react (and dimerise) more slowly, and the corresponding dimers are consumed slowly. Type III alkenes are still reactive in CM, but will not dimerise. Type IV alkenes do not react, but will not poison catalysts, and therefore act as 'spectators'. Categorising each CM partner for a given reaction allows the outcome to be predicted. The category into which a given motif falls is a function of the pre-catalyst, with different behaviour observed for molybdenum complexes, and for first- and second-generation ruthenium complexes. Notably, the reactivity of second-generation complexes varies considerably, depending on the nature of the dissociating ligand and on the identity of the NHC ligand. For example, complexes bearing less hindered NHCs have been utilised to prepare heavily-substituted alkenes, such as in Stoltz's synthesis of (+)-elatol, where complex **10** enabled the preparation of the challenging tetrasubstituted cyclohexene unit (Scheme 9).[72]

For this reason, there is no universal 'best' catalyst,[73] and research is currently underway in a number of laboratories to develop new catalysts and apply these to otherwise challenging or impossible substrates and reaction conditions.

The degree of thermodynamic control in a metathesis reaction will also depend on the pre-catalyst system; the issue of thermodynamic control has been reviewed recently by Fogg *et al.*[74] Second-generation catalyst systems can react with starting materials (*i.e.* typically monosubstituted alkenes) and products (typically 1,2-disubstituted alkenes),[54] so can more easily approach the thermodynamic end point of a reaction. This was demonstrated experimentally by Percy and co-workers, who showed that the RCM of 1,8-nonadiene (using different loadings of **G2**) and the ROMP of cycloheptene (in the presence of ethene) led to the same equilibrium mixture.[75] It was also evident when Grubbs *et al.* explored the development of a system for pre-catalyst characterisation, using a number of model reactions.[76] In a prototypical benchmark reaction (Scheme 10), second generation catalysts achieved better *E*/*Z* selectivities in shorter periods of time than first generation species (Fig. 4). The *E*/*Z* selectivity of a metathesis reaction is a key outcome that will affect the viability of a process. While RCM to form smaller (*ca.* 5–8 membered) rings almost[77] always produces *Z*-alkenes, CM reactions and RCM reactions to produce larger rings (such as macrocycles)[78] can yield the *E*- or *Z*-isomer.

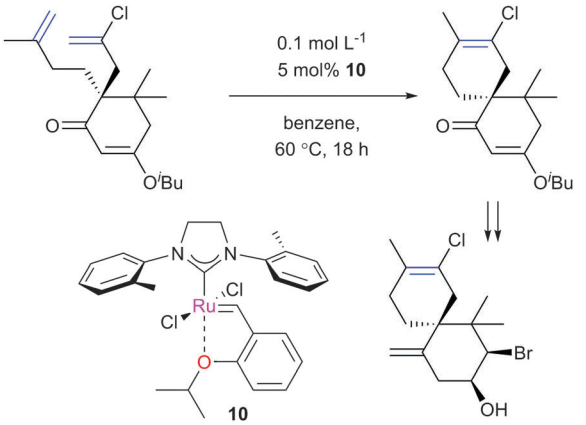

Scheme 9 Stoltz's synthesis of (+)-elatol.

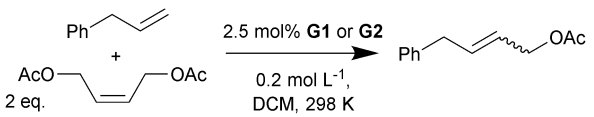

Scheme 10 A prototypical cross-metathesis reaction.[76]

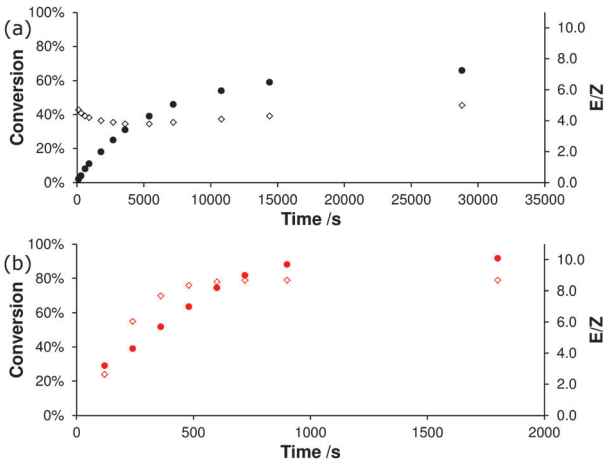

Fig. 4 Conversion to product (closed circles) and *E*/*Z* ratio (open diamonds) *versus* time for the reaction in Scheme 10 with (a) 2.5 mol% **G1** or (b) 2.5 mol% of **G2**.[76]

A fuller discussion of *E*/*Z* selectivity can be found in a subsequent section of this manuscript.

Several studies have sought to explain the reactivity differences between first- and second-generation catalysts. Cavallo explored the early stages of metathesis with a series of complexes, from initiation to MCB formation, in one of the first DFT studies of metathesis that considered untruncated structures (Scheme 11).[79] Calculations on the MCB formation step showed that second generation complexes (**N2** and **G2**, bearing IMes and SIMes, respectively) face lower barriers than first generation **G1**, and yield MCBs that are lower in energy. In addition, the steric pressure exerted by the (S)IMes ligands destabilised the phosphine-bound and olefin-bound intermediates, leading

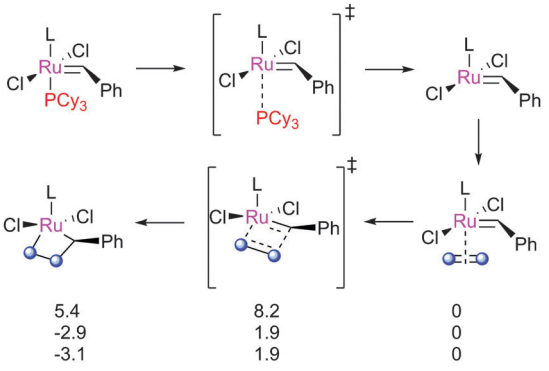

Scheme 11 Structures explored by Cavallo.[79]

to more energetically favourable metathesis but not increased initiation rate.

Straub conducted calculations on methylidene complexes **11** and **12**, and the four conformers of their η^2-complexes with ethene.[80] In the reactive conformer, the alkene and the carbene are in the same plane, and aligned in the same direction (Fig. 5). For second-generation complexes, the energy difference between reactive and unreactive conformers was smaller than for first-generation complexes, explaining the observed reactivity differences. Attempts to optimise the structure of the reactive conformer led to MCB formation. A later study evaluated the bonding in active ruthenium carbene complexes to rationalise the effect of the NHC on their stabilisation.[81] In common with other DFT studies (*vide infra*), it was shown that second-generation MCBs are relatively low in energy, as opposed to the first-generation MCBs which are relatively high in energy and have not been observed spectroscopically.[46] The pathway proceeding *via cis*-dichloride intermediates (*i.e. via* side-bound MCBs) was shown to be far less favourable.

Lavigne *et al.* proposed that through space π–π* interactions between the aryl moiety on the NHC and the ruthenium carbene stabilise NHC-bearing complexes.[82] Plenio and co-workers used electrochemical measurements to show their existence.[83,84] Cavallo and co-workers have shown that, for transition metal complexes in general, there exist interactions between the aryl rings of bis(aryl)-NHCs and the transition metal d-orbitals.[85] The electron density of these aryl rings can therefore modulate

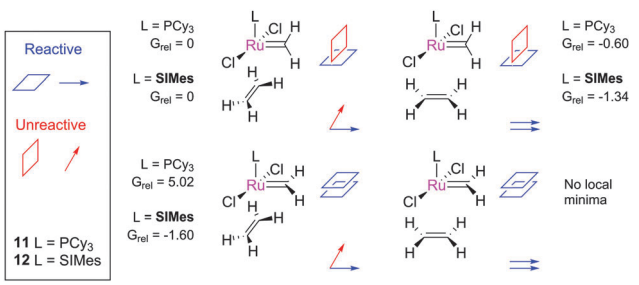

Fig. 5 The four conformers of the complex between methylidene and ethene; relative energies are in kcal mol^{-1} using the B3LYP density functional.[80]

this interaction. This is, of course, an interaction that is not available in first generation complexes.

Metathesis catalysts can react with alkynes and allenes, as well as alkenes, allowing elaborate cascade reactions. Sohn and Ihee used time-dependent fluorescence quenching studies to explore the affinity of metathesis catalysts for alkenes, allenes and alkynes. During enyne metathesis, **G1** favoured reaction with the alkene terminus first.[86] In a subsequent study, molybdenum complexes were shown to favour alkyne over alkene over allene, while first generation ruthenium complexes favoured allene over alkene over alkyne.[87] Second-generation ruthenium complexes favoured alkyne over allene over alkene. Understanding this order of selectivity is important in the design of cascade metathesis reactions.

The use of NHCs as ligands for metathesis pre-catalysts has allowed access to a vast range of interesting catalyst structural motifs, each with different reactivity.[6,7] Such ligands can be prepared using a variety of established and scalable organic synthetic chemistry methodology.[88] While monodentate phosphine ligands sterically influence the metal centre in a limited number of ways (measured using the concept of 'cone angle'),[55] NHCs can be constructed from various organic scaffolds and can therefore influence the steric environment of the metal in various ways. These differences are best quantified using the percent buried volume (%V_{bur}) metric, which quantifies the percentage of the volume of a sphere (typically of 3.5 Å radius) occupied by the ligand.[89] Steric maps which describe how various sections of the co-ordination sphere are occupied can also be constructed,[90] using the freely-available online SambVca tool.[91] The electronic properties of the range of NHCs known can also be quantified and compared.[24,92]

Detailed studies have therefore shown that the reactivity difference between first- and second-generation complexes lie in the metathesis steps as well as in the initiation pathways. More favourable MCB formation in particular leads to an enhancement of catalytic performance. The highly flexible NHC scaffold has allowed for a wide variety of complexes to be prepared; for example, *N*-alkyl-*N*-aryl-bearing NHCs have found application as selective ethenolysis catalysts,[93] and in the preparation of small cyclic oligomers instead of long-chain polymers.[94] More novel complexes with new and interesting reactivities will surely follow in years to come.

Partitioning between intra- and inter-molecular pathways

As all alkene metathesis reactions proceed *via* the same basic [2+2]cycloaddition mechanism, using the same functional groups, catalysed by the same active species, different processes may sometimes compete. CM reactions seek the selective coupling of two different alkene partners, and therefore the challenge lies in this selectivity. In contrast, the RCM reactions of dienes can be complicated by competing CM processes to produce dimers or polymers. An understanding of the kinetics and thermodynamics of these processes can help mitigate the impact of these deleterious reactions on RCM.

While the concept of effective molarity (EM)[95,96] (Scheme 12) has been applied widely in the study of acid- and base-catalysed

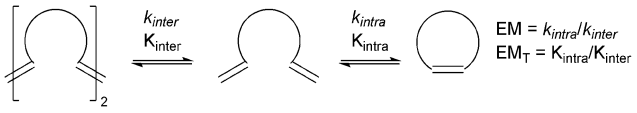

Scheme 12 Effective molarity to measure cyclisation efficiency.

nucleophilic ring-closing chemistry, there are relatively few examples of this concept in metathesis chemistry. Fogg *et al.* have probed the competition between intra- and intermolecular metathesis in some model reactions, and tabulated EM ranges for some compounds from the literature.[97] Many of these ranges are broad, and are for *cycloalkanes* rather than cycloalkenes, which will have different EMs;[98] none are for RCM. The authors also proposed that oligomeric material is an intermediate in the preparation of medium (7, 8 and 9-membered) rings. However, metathesis catalysts can be difficult to quench; careful treatment of samples is necessary to deactivate the catalyst, as concentration and analysis (by GC) while the catalyst is still active will lead to an effective increase in the reaction concentration and misleading data on the degree of conversion and oligomerisation.[99] Later studies, where high resolution (600 MHz) NMR spectroscopy was employed to follow the reactions of simple prototypical α,ω-dienes with **G2** (Scheme 13),[100] did not detect the behaviour reported by Fogg. Instead, slow oligomerisation competed with ring-closing.

Percy *et al.* showed that the metathesis reactions of these simple substrates are under thermodynamic control;[75] metathesis of the products yielded the same final mixture as metathesis of the substrates. Importantly, it was shown that the reaction outcomes were predictable, using thermodynamic data available in the literature[98,101] or from DFT calculations (Table 3). In this manner, the optimal initial reaction concentration can be selected on the basis of straightforward calculations, rather than by expensive and time-consuming trial and error. The ratio of intra- to intermolecular products also depends on the degree of thermodynamic control. In the example above, the ring-opening of strained cycloalkenes is typically fast, allowing the reaction to reach a thermodynamic end point within hours. For reactions where product ring-opening is slow, the final ratio of cyclic product to oligomer will depend predominantly on the *rate* of the formation of each species. In contrast, where reactions are under thermodynamic control, the same equilibrium position will be achieved regardless of whether this position is approached from the substrate or from the product.

The partitioning between intra- and intermolecular metathesis is therefore a function of the pre-catalyst and substrate structure. While some studies have been conducted there remains considerable scope for further understanding of these factors, and the use of this understanding in the design of new pre-catalysts and synthetic reactions.

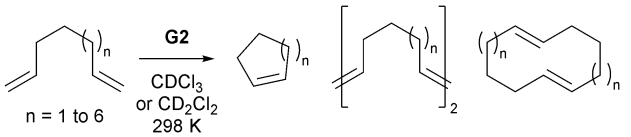

Scheme 13 RCM of simple prototypical diene substrates.

Table 3 Calculated *versus* measured thermodynamic effective molarities for simple cycloalkene compounds

Ring size	5	6	7	8	9	10
$\log_{10}(EM_T^{DFT})^a$	−0.78	1.75	−1.25	−3.35	−5.90	−3.87
$\log_{10}(EM_T^{DFT})^b$	−0.63	1.52	−2.52	−3.31	−6.24	−3.48
$\log_{10}(EM_T^{DFT})^c$	−0.27	≫0.60	−1.28	−3 to −4	<−4	<−4

[a] From DFT calculations (M06-L/6-311G**) with 6 kcal mol^{-1} added to ΔG_{RCM} (see ref. 75). [b] From an empirical treatment[98] of literature data. [c] From a series of small scale metathesis experiments, by ^{1}H NMR.

Study and understanding of key processes and intermediates

Several groups have applied ESI-MS techniques to study metathesis reactions in the gas phase. Reaction mixtures are passed into the mass spectrometer, allowing the various products and intermediates to be identified and manipulated. The Chen group have contributed a great deal in this area. In the first report, **13** (bearing ionically-tagged phosphines) underwent phosphine dissociation in the spectrometer to yield 14e$^-$ species **14**.[102] Such 14e$^-$ species have, despite advanced low temperature NMR studies (*vide infra*), never been observed in the solution phase. The reactions of **14** with substrates such as 1-butene and norbornene were probed, with strained cycloalkenes undergoing reaction more quickly: norbornene underwent reaction 15-fold faster than 1-butene, and 1500 times faster than cyclopentene. The direct detection of the 14e$^-$ species is one of the major advantages of this method, although modified species bearing ionic tags are necessary.[103]

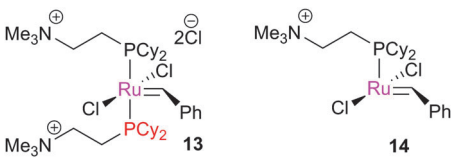

Subsequently, these experiments were compared to DFT calculations.[104] Various complexes were prepared in the spectrometer, and subjected to reaction with 1-butene or norbornene (Scheme 14). Electron-withdrawing substituents accelerated the reaction with 1-butene ($\rho = 0.69 \pm 0.10$). Subsequent experiments probed the reversibility of the reaction; **15** underwent ring-opening followed by ring-closing when exposed to **16**, to generate **17** (Scheme 15). The corresponding cyclopentane substrate was unreactive. DFT calculations, using the highly truncated model system $[RuCl_2(PH_3)_2(CH_2)]$ to represent $[RuCl_2(PCy_2(CH_2CH_2NMe_3))(CH_2)]^+$, showed that the MCB was higher in energy than the η^2-complex, and that the *cis*-chloride MCB complex was lower in energy than the *trans*-isomer, but kinetically inaccessible. PH_3 is a simple phosphine, so this energy difference between isomers is likely to be different in systems with a bulky trialkylphosphine.

Subsequent studies explored other themes. The activity of complexes **18**, **19** and **20** in the gas phase were compared, and

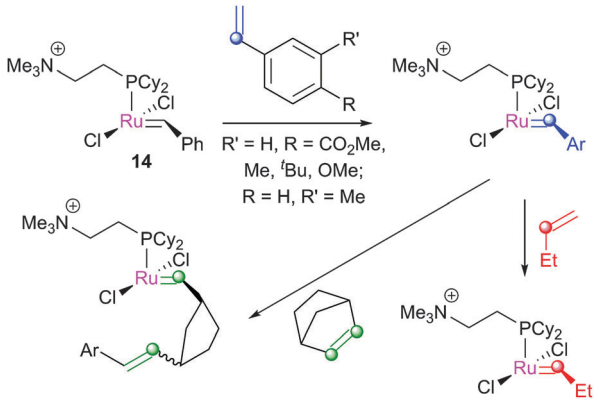

Scheme 14 Probing the reactions of various substrates with 14e⁻ species **14**.

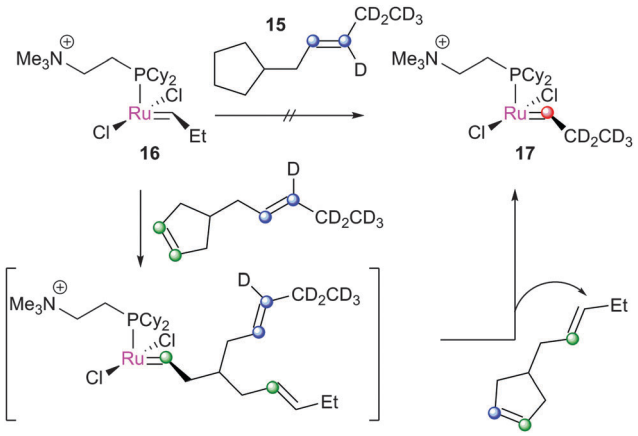

Scheme 15 Probing the reversibility of alkene metathesis.

found not to reflect those in solution; the authors suggested that this is due to the equilibrium in place before the active complex is generated, highlighting the need to understand the initiation behaviour of these complexes.[105]

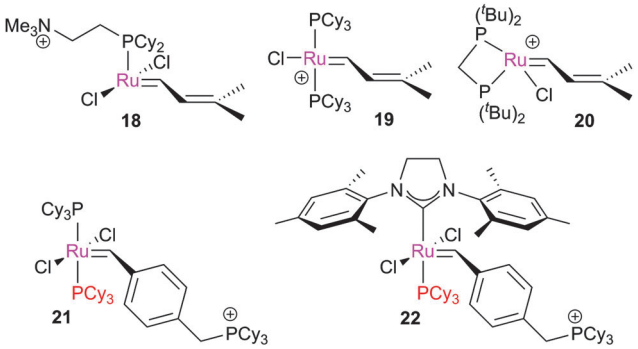

These studies continued to develop more detailed and informative techniques. In a study of **21** and **22**, bearing cationic benzylidene ligands, variation of the collision energies allowed the energetic landscape of the reaction of these complexes with norbornene to be probed.[106] Excellent agreement was achieved with DFT studies,[31] where the M06-L/TZP-CP level of theory was used; BP86/ZORA-TZP led to much poorer agreement.

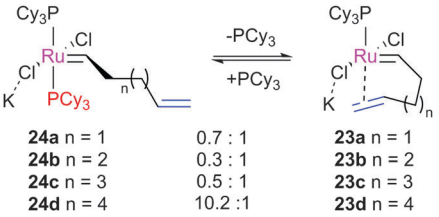

Scheme 16 The equilibrium between chelated η^2-complexes and phosphine-bound alkylidenes.

Metzger has been active in this area, detecting the products of reactions of complex **G1** with ethene and prototypical RCM substrates. Intermediates throughout the catalytic cycle were detected.[107] A subsequent study quantified the relative rates of RCM of some simple dienes (see Schemes 11 and 16), where 1,7-octadiene reacted fastest, followed by 1,6-heptadiene and 1,8-nonadiene at approximately equal rates.[108] Further, the equilibrium between chelated η^2-complexes **23** and phosphine-bound alkylidenes **24** was probed (Scheme 16); the latter must first dissociate the phosphine before MCB formation from the chelated η^2-complex can occur. Surprisingly, 1,5-hexadiene-derived complex **23a** was considerably more stable than the phosphine-bound species. Later studies by Ashworth *et al.* established *via* DFT studies that the chelated complex was very stable, due to favourable interactions and a lower entropic penalty for cyclisation than longer dienes, in which more rotors must be frozen.[100] 1,6-Hexadiene had an *inhibitory* effect on the metathesis of 1,6-heptadiene and 1,7-octadiene.

The majority of studies have been conducted with first generation systems, as rapid phosphine dissociation allows quick generation of interesting intermediate carbene species. The study of alkali metal adducts of metathesis catalysts precludes the requirement for the time-consuming synthesis of modified complexes with ionic functionality. While these techniques have been applied to some studies of second generation carbene complexes,[106] and most recently to studies of pre-catalyst initiation,[109] there is further scope to investigate the reactivity of ruthenium carbene complexes using this approach.

A significant advance was made when Piers and co-workers developed rapidly-initiating 14e⁻ ruthenium carbene complexes such as **Piers1** and **Piers2**.[17,18,49] While the rapid, irreversible generation of large quantities of 14e⁻ carbenes (on reaction with ethene) renders these species non-ideal for longer reactions where decomposition may adversely affect performance, they have found application in mechanistic studies, particularly as heteroleptic NHC–phosphine complexes initiate slowly.[25] This class of compound has enabled the preparation, observation and study of MCB species using modern low-temperature NMR spectroscopic techniques.[46] In the first report of this reactivity, Piers demonstrated that the reaction of **Piers2** with 2.2 equiv. of ethene yielded quantitative conversion to parent MCB **25** (Scheme 17). The NMR data suggested a bottom-bound MCB, while H_α exhibited a resonance at 6.6 ppm and H_β at −2.6 ppm.

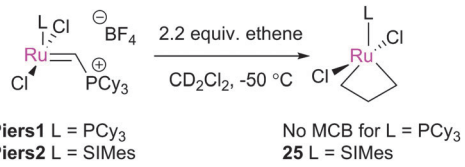

Scheme 17 Formation of MCBs using Piers-type complexes.

$^1J_{CH}$ coupling constants suggested a 'kite-shaped' MCB. First generation analogue **Piers1** yielded no observable MCB, consistent with DFT calculations that suggest that first generation MCBs are less stable than their second generation analogues.[79]

Further studies from the Piers and Grubbs groups followed. Grubbs *et al.* studied the reaction of Piers-type complexes with ethene and propene.[51] This study established that MCBs where the two *N*-substituents of the NHC were different (such as **26**) exhibit two resonances for H_α protons, indicating slow rotation of the NHC (*i.e.* on the NMR timescale). The bottom-bound nature of the MCB was also confirmed. In addition, 2D [^{1}H, ^{1}H] EXSY spectroscopy enabled the measurement of the rate of degenerate exchange between the α- and β-positions *via* MCB breakdown, ethene rotation, and MCB formation ($k = 26 \pm 2\ s^{-1}$, corresponding to $\Delta G^{\ddagger} = 12.2$ kcal mol^{-1} at 233 K).

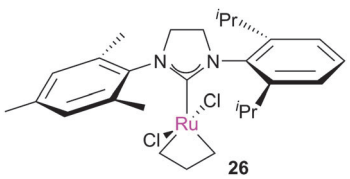

The Piers group probed the reactions of this MCB species in detail.[47] Exchange with free ethene-$^{13}C_2$ was much slower than intramolecular α/β-exchange ($k = (4.8 \pm 0.3) \times 10^{-4}$ L mol^{-1} s^{-1}), suggesting that ethene binding or unbinding events presented significant barriers. Interestingly, determination of the thermodynamic parameters for this intermolecular reaction ($\Delta H^{\ddagger} = 13.2 \pm 0.5$ kcal mol^{-1}; $\Delta S^{\ddagger} = -15 \pm 2$ cal K^{-1} mol^{-1}) suggested an associative mechanism for the exchange; ethene is the smallest possible olefin, and therefore it is possible that the metal centre might be able to co-ordinate two ethene molecules.

Webster has carried out calculations to probe degenerate ethene exchange.[110] Initial calculations on intramolecular ethene exchange produced results consistent with the aforementioned experimental studies. Bottom-bound MCBs bearing *trans*-chloride ligands provided the lowest energy pathway; the calculated barrier for the exchange ($\Delta G^{\ddagger}$ (DCM, 227 K) = 14.4 kcal mol^{-1}) was in excellent agreement with the measured value. The calculated pathway for associative ethene exchange (Fig. 6) features octahedral six co-ordinate intermediates between the two MCBs with TSs for MCB formation and breakdown where twisting of the ethene ligand (to render it parallel to the Cl–Ru–Cl vector) is concomitant with C–C bond cleavage and C=C bond formation. The involvement of a six co-ordinate metallacyclohexane was ruled out. The calculated barrier for this process ($\Delta G^{\ddagger}$ (DCM, 227 K) = 18.6 kcal mol^{-1}) was in excellent agreement with experiment ($\Delta G^{\ddagger}$ (DCM, 227 K) = 16.9 kcal mol^{-1}). These results

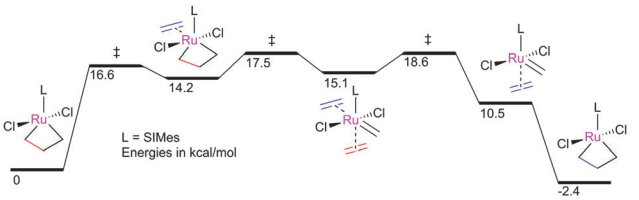

Fig. 6 Potential energy surface for an associative, intermolecular exchange of ethene in **25**.

raise questions about the involvement of high-energy four co-ordinate 14e ruthenium carbene intermediates; however, this example covers only the case of ethene, which is a particularly unhindered substrate, so more hindered substrates may behave differently.

Piers and co-workers subsequently examined the ring-closing metathesis of diethyl diallylmalonate using complex **Piers2**, wherein complex **27** was detected spectroscopically.[48] While generated from the reaction of MCB **25** with *gem*-disubstituted cyclopentene **28** (Scheme 18), this intermediate is formally the product MCB from the metathesis of diethyl diallylmalonate. This intermediate undergoes reversible retro[2+2]cycloaddition to yield propagating carbene species **29**, which was trapped by the addition of PMe_3 to yield complex **30**. In addition, the ring-opening of acetonaphthalene could be achieved in the presence of ethene, forming the corresponding ruthenium carbene complex.[48] Other closely related MCBs relevant to RCM chemistry could be prepared; alkenes such as cyclohexene, 3,3-dimethylbut-1-ene, and 1,1-difluoroethene did not generate the corresponding MCBs, however. The ^{13}C chemical shifts and proposed structures were later confirmed by DFT calculations;[111] the Ru–C_β interaction was proposed to be the cause of stabilisation of the MCB, with a bond order of *ca.* 0.3.

Piers later published a detailed study of RCM using low-temperature NMR techniques,[50] in which the PES of the reaction at 220 K was mapped by measuring key rate constants. Such detailed mapping of the PES typically requires theoretical tools rather than experimental ones, so the provision of experimentally measured energies is exciting. This work suggests that MCBs may well function as 'protecting groups' for the high-energy, fragile 14e ruthenium carbene complex.

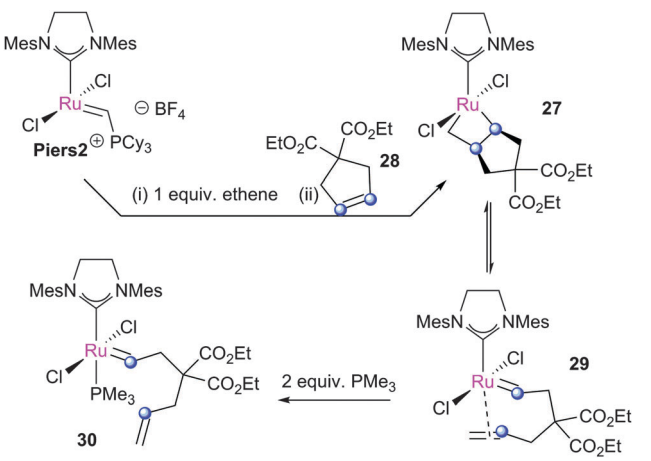

Scheme 18 Formation and trapping of a MCB of relevance in RCM.

A full paper was published by Grubbs in 2011,[52] where **Piers2** underwent reaction with propene, 1-butene and 1-hexene to yield the corresponding MCBs. The composition of the MCB mixture varied with time and temperature, which was proposed to be driven by the loss of ethene; parent MCB **25** was favoured initially, while *trans* and *cis* α,α′-disubstituted MCBs were in equilibrium (*e.g.* 2.5 : 1 **31** : **32**). Surprisingly, no β-substituted MCBs were obtained, even when 1,2-disubstituted alkenes were employed, suggesting that these are higher in energy.

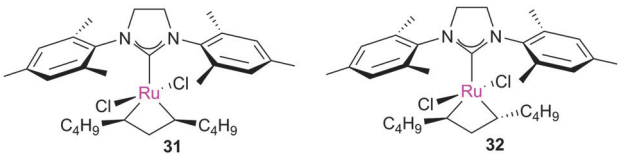

MCBs derived from unsymmetrically-substituted NHCs have been studied.[53] The investigation of these complexes revealed varying rates for degenerate ethene exchange with different catalysts and, most intriguingly, that the de-binding rate of the cycloalkene was much lower than in complexes bearing, for example, SIMes. While these results were obtained at conditions far from those used in synthetic laboratories, this observation suggests that slow product de-binding may allow for more non-productive cycles per productive cycle, and therefore slower metathesis overall. Further, this observation is relevant to the proposal by Solans-Monfort and co-workers that the alkene de-binding step may play an important role in the initiation of Hoveyda-type metathesis catalysts.[40]

Grubbs *et al.* investigated the relative ratio of non-productive to productive cycles for a range of pre-catalysts in the solution phase under typical synthetic RCM conditions.[112] The metathesis of diethyl diallylmalonate-d_2 yields the corresponding cyclopentene from productive metathesis, while diethyl diallylmalonate-d_0 and -d_4 result from non-productive metathesis (Scheme 19). Common pre-catalysts such as **G2** and **GH2** performed 10 productive cycles per non-productive cycle, while pre-catalysts bearing unsymmetrical NHCs (*e.g.* **33**) performed as many (or more) non-productive as productive cycles. These differences were proposed to be due to the differing steric environments in these types of complexes. While many intermediates are not observable under typical experimental conditions in the solution phase, a number of elegant experiments have been utilised to probe equilibria and processes occurring in metathesis reactions.

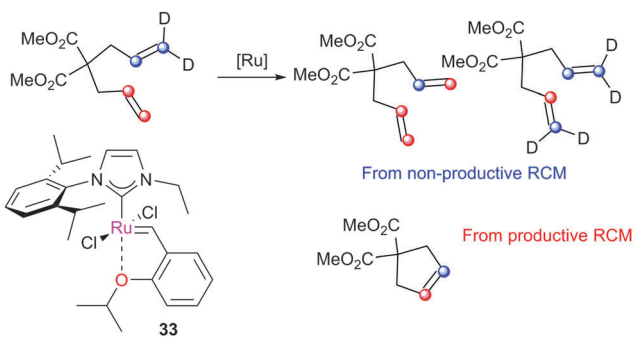

Scheme 19 Probing non-productive processes in RCM.

Grubbs *et al.* investigated the effect of alkylidene structure on reactivity with 1-alkenes using kinetic studies of first-generation **G1** and derivatives.[113] Bulky alkenes were found to react slowly (or not at all); 3,3-dimethylbut-1-ene, 2-methylpent-1-ene and 1-phenylprop-1-ene were poorly reactive.

Lane *et al.* examined the effects of alkene structure on the formation of ruthenium carbene complexes.[114] Complexes were prepared from the reaction of **G1** with a range of alkenes. Equilibrium was established in each case, with a wide range of constants (Table 4; for larger 1-alkenes, K_{eq} tends to *ca.* 0.3, and ΔG to *ca.* 0.7 kcal mol^{-1}). Steric and electronic properties play a role, with smaller, electron rich alkylidenes being preferred. A good correlation was obtained for the free energies of reaction

Table 4 Equilibrium constants K_{eq} for the reaction of **G1** with various substrates[114]

Entry	Substrate	K_{eq}	ΔG (kcal mol^{-1})
1	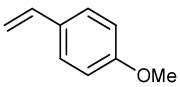	8.66	−1.26
2	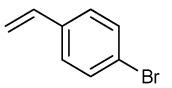	1.10	−0.056
3	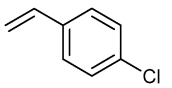	1.25	−0.129
4	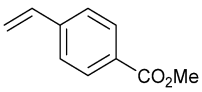	0.367	0.584
5	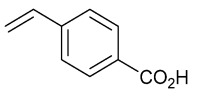	0.295	0.684
6		8.66	−1.251
7		1.76	−0.326
8		0.34	0.624
9		0.00188	3.68
10	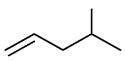	0.128	1.21
11	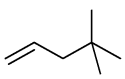	0.0148	2.47
12	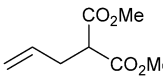	0.172	1.03
13	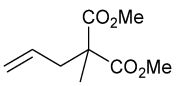	0.00455	3.14
14	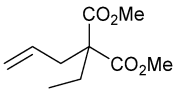	0.00210	3.60

versus a linear combination of Hammett σ_r and σ_i parameters ($\Delta G = (0.90\cdot(2.7\cdot\sigma_r + \sigma_i) - 0.0036)$ kcal mol^{-1}). For particularly bulky alkenes, such as those bearing quaternary homoallylic positions, the reaction was very unfavourable with K_{eq} as low as 10^{-3}. These results may explain why the RCM reaction of diethyl diallylmalonate occurs slower than that of 1,6-heptadiene,[115] despite the clear thermodynamic preference of the diethyl diallylmalonate to undergo ring closing.

Grubbs and co-workers prepared and studied model compound **34**, in conformations **a** and **b**.[116] Surprisingly, *trans*-**34** was not observed; crystalline material obtained was composed of *cis*-**34a**, which provided *cis*-**34b** on heating. This process was under thermodynamic control, with higher temperature favouring *cis*-**34b**. Detailed NMR experiments confirmed the assignments. Piers and co-workers have characterised a related example from the ring-opening of acenaphthylene.[48] These are particularly rigid examples of chelated alkylidenes; Snapper and co-workers have previously isolated and characterised *trans*-dichloride chelated alkylidene **35**, based on a 1,2-divinylcyclobutane motif;[117] the structural effects which decide if *cis*- or *trans*-isomers are favoured in solution are therefore likely to be somewhat subtle.

A subsequent detailed study evaluated more complexes.[118] The dynamic solution behaviour varied; for **36**, no exchange between the two *cis*-isomers occurred at room temperature. The SIPr complex showed strong preference for the isomer in which the terminal CH_2 is directed towards the NHC (analogous to **37**), while chiral complexes such as **38** did not undergo exchange. Complexes bearing PCy_3 in place of an NHC underwent exchange. When a bulkier olefin, 1-vinyl-2-(2′-methylethenyl)benzene was used in place of 1,2-divinylbenzene, NHC rotation was observed to occur, but not exchange between η^2-isomers. These experiments provide insight into dynamic solution behaviour that is difficult to probe using static methods such as X-ray crystallography. A third study evaluated the behaviour of complexes derived from the reaction of **39** with 1,2-divinylbenzene; DFT calculations agreed with the observed solution behaviour with regards to the proportions of each conformer that were observed.[32]

Plenio explored the postulated 'release-return mechanism'[14,15] in reactions catalysed by pre-catalysts such as **GH2**.[119] Hoveyda and co-workers had successfully isolated a proportion of **GH1** from metathesis reactions, and therefore reasoned that the chelating iso-propoxystyrene ligand must return to the metal centre after reaction. However, Plenio and co-workers studied reactions catalysed by fluorescence-labelled **40** and fluorine-tagged **41**, and did not observe the return of the ether ligand. The authors proposed that the recovered complex was uninitiated pre-catalyst; concentration/time data for the RCM of diethyl diallylmalonate reported by Percy *et al.* was later reported where complete conversion was obtained when only a fraction of the pre-catalyst had undergone initiation.[115] Recent work by Solans-Monfort and co-workers supports this view.[120]

E/*Z* selectivity is key in metathesis: one isomer is typically desired in synthetic applications, while in polymer chemistry selectivity is necessary for a regular repeating structure. *E*/*Z* selectivity in CM reactions can be linked to several factors.

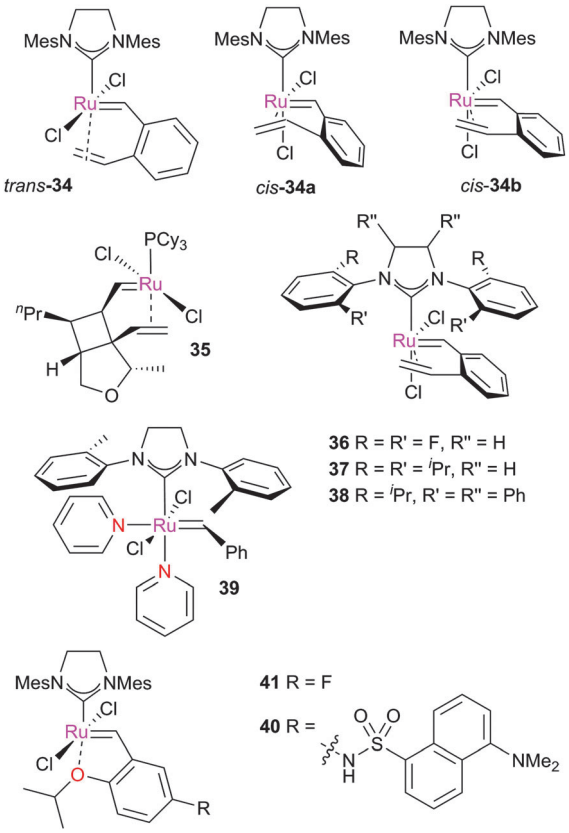

As discussed above, second-generation pre-catalysts tend to lead to higher *E*-selectivities in CM reactions,[76] due to their ability to equilibrate *E*/*Z* mixtures of products to the thermodynamically-favourable *E*-isomer. The structure of the ligands of second generation pre-catalysts can affect the *E*/*Z* ratio;[121,122] for NHC–phosphine complexes, this ratio is typically *ca.* 3–10 (or higher), while for bis(NHC) complexes it can be *ca.* 2.

In RCM reactions, the thermodynamic product (*E* or *Z*) will depend on the structure of the product. For common and medium rings (5–10 members) the *cis*-isomer is typically preferred, due to the vast difference in strain energy between the *cis*- and *trans*-isomers.[101] There are few examples of *trans*-configured eight-membered rings. Prunet and co-workers reported the preparation of *trans*-**42** *via* RCM of substrate (*S*)-**43** (Scheme 20);[77] corresponding (*R*)-**43** was unreactive. This appears to be an isolated example of where dense functionalisation renders the *trans*-isomer more favourable than the *cis*-isomer; the fused cycloalkene and carbonate, plus the heavy substitution of

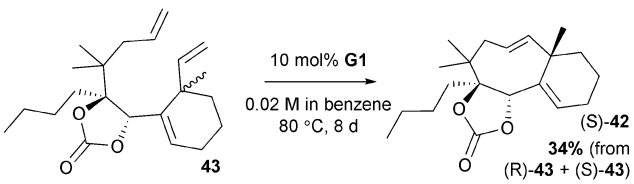

Scheme 20 Synthesis of a *trans*-cyclooctene motif by RCM.

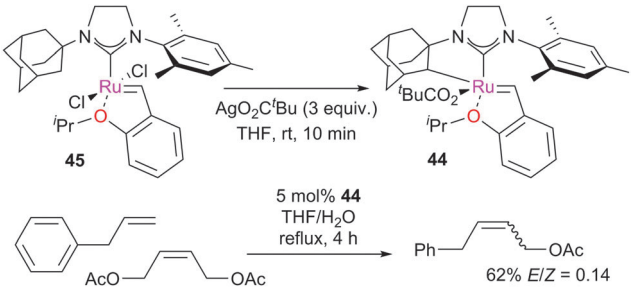

Scheme 21 *Z*-selective metathesis.

most positions around the ring, clearly influences the energetics of the ring-closing reaction.

A key development in metathesis has been the design of *Z*-selective catalysts.[123,124] Hoveyda and Schrock reported molybdenum- and tungsten-based *Z*-selective catalysts in 2009,[125,126] while Grubbs reported the first ruthenium-based *Z*-selective catalyst **44** in 2011 (Scheme 21).[127] **45**, bearing an unsymmetrical 1-adamantyl-3-mesityl-substituted NHC, underwent reaction with AgO_2C^tBu to yield cyclometallated complex **44**. When tested in the CM reaction of allylbenzene with acetyl-protected but-2-ene-1,4-diol, **44** led to *E*/*Z* ratios as low as 0.14. However, **44** was shown to be far slower for the RCM of diethyl diallylmalonate than **GH2**, even at higher temperatures and with much higher catalyst loadings.

In a subsequent study, the effect of the pre-catalyst structure on reactivity was examined.[128] Complexes such as **46**, bearing chelating unsymmetrical NHCs and bidentate κ^2-nitrato ligands were found to be the most active, achieving modest to excellent yields and *E*/*Z* ratios of typically 0.25 or lower. Studies suggested that a bulkier ligand sphere increased the initiation rate of the catalyst. This result, combined with the octahedral coordination sphere of the metal centre, suggests that an interchange or associative mechanism is unlikely, and that a dissociative mechanism is in operation for initiation.

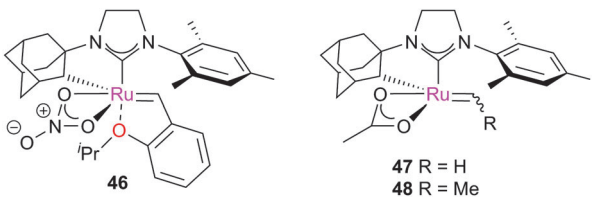

Computational studies have been carried out in order to investigate why the chelate nature of the NHC and the replacement of the halide ligands stimulates a switch in selectivity from *E* to *Z*. Houk *et al.* investigated the reactivity of model $16e^-$ species **47** and **48** with ethene and propene.[129] Calculations of the degenerate exchange of ethene with **47** revealed that the chelated complexes strongly preferred the side-bound reaction, in contrast to **G2**.[130] This is due to the chelating adamantyl substituent, which renders complexes where the alkylidene is *trans*- to the Ru–C σ-bond highly unfavourable, and introduces steric repulsion in the TSs for bottom-bound (retro)metallacyclobutanation. Side-bound TSs suffer far less steric repulsion, and $d–\pi^*_{NHC}$ and $d–\pi^*_{alkylidene}$ back-donation can occur *via* different, perpendicular d-orbitals. Side-bound MCBs were found to be far more stable (*versus* **47**, ΔG = −7.3 (side-bound), + 9.4 (bottom-bound) kcal mol^{-1}). Consideration of the metathesis of propene with **48** revealed that side-bound MCBs were favoured; in these intermediates, TSs leading to the *Z*-olefin ($\Delta G^{\ddagger}$ = 14.4 and 14.6 kcal mol^{-1}) were more favourable, as these allowed both methyl groups to point downwards, away from the bulky NHC, while the *E*-selective TSs ($\Delta G^{\ddagger}$ = 16.1 and 18.8 kcal mol^{-1}) require at least one methyl group to be orientated towards the NHC.

Additional computational studies regarding this selectivity have been conducted by Wang *et al.*, who considered more steps of the mechanism.[131] The initiation event was modelled according to the originally proposed dissociative mechanism,[26,40,132] due to the coordinatively-saturated nature of the ruthenium centre (*vide supra*); interchange and associative pathways[37–39] were not considered. Dissociation was followed by facile isomerisation of the square-based pyramidal complex **49** to trigonal bipyramidal complex **50**, which was considered as the active species. The various pathways *via* which the reaction can proceed were modelled in detail; while the *E*-isomer was favoured thermodynamically, the kinetics favour *Z*-isomer formation. The authors confirmed that, while there were several other TSs on the PES, the key TS involves retro-[2+2]-cycloaddition to break up the MCB intermediate, where steric interactions with the NHC ligand are key. A later study confirmed that nitrato-analogues of these catalysts function in a similar way,[133] with the ability of the ligand to switch between mono- and bi-dentate coordination modes key to the activity.

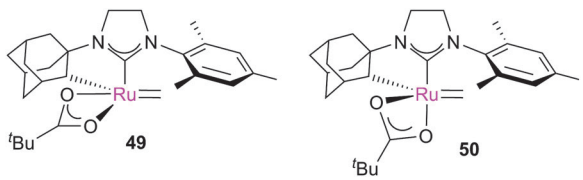

More recently, Jensen and co-workers disclosed the synthesis and study of an accessible *Z*-selective metathesis pre-catalyst. Simple exchange of a chloride ligand on **GH2** with an arylthiol potassium salt led to complex **51**, which showed excellent *Z*-selectivity (Scheme 22).[134] Similarly, Hoveyda and co-workers have developed a different approach using the 2,3-dimercaptomaleonitrile ligand which, due to the forced

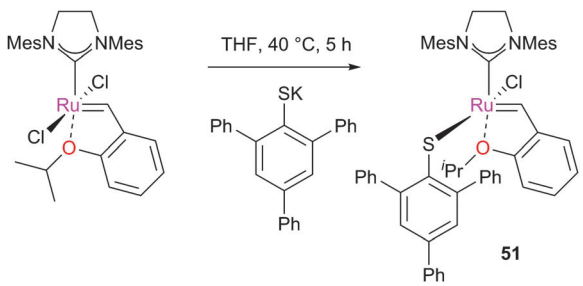

Scheme 22 Synthesis of a simple *Z*-selective metathesis catalyst.

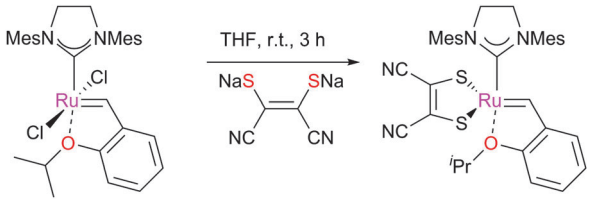

Scheme 23 Synthesis of a simple *Z*-selective metathesis catalyst.

cis-anion conformation, promotes the formation of *Z*-olefins in high selectivity and yields (Scheme 23).[136]

A DFT study on the stereochemical processes occurring around various types of (a)chiral ruthenium carbene complexes has recently carried out by Hoveyda *et al.*[135,136] Their calculations indicated that the typical preference for bottom-bound MCBs was a consequence of destabilising the side-bound alternative (which will have *cis*-anionic ligands) *via* electron–electron repulsion and a large dipole moment. Ligand spheres which destabilise the usual square-based pyramidal geometry of metathesis catalysts can favour side-bound MCBs and therefore *Z*-selective metathesis. In chelated NHC complexes such as **46**, the other anionic ligand is proposed to prefer to be *trans* to the NHC rather than the alkyl ligand, favouring a side-bound MCB.

Catalyst decomposition

Designing and utilising ligand environments that reduce deactivation pathways is always one of the major challenges in organometallic chemistry. However, to develop new and more efficient catalysts, understanding the decomposition processes is fundamentally important. Chemists seek to understand why side products may be formed during complex synthesis and during metathesis reactions, and also to evaluate the compatibility of catalysts with different chemical environments (*e.g.* to understand catalyst deactivation). In addition several catalyst decomposition products can react with metathesis substrates; therefore, it is very important to understand what these complexes are and which reactions they can catalyse.

Methylidene complexes

Methylidene complexes, formed after catalytic turnover with terminal alkenes, are often viewed as the most fragile species in metathesis reactions. During propagation, species **11** and **12** can re-coordinate the phosphine ligand, forming the corresponding 16e$^-$ methylidene species **52** and **53** (Scheme 24).

Even though **52** and **53** are not formally decomposition products, they are prone to rapid decomposition, to the extent that their initiation rates cannot be measured.[25] Their instability was proposed by Grubbs *et al.* to be due to rapid decomposition

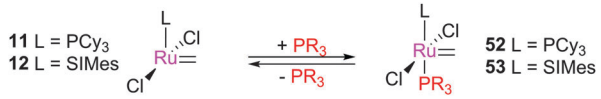

Scheme 24 Phosphine capture of methylidene complexes.

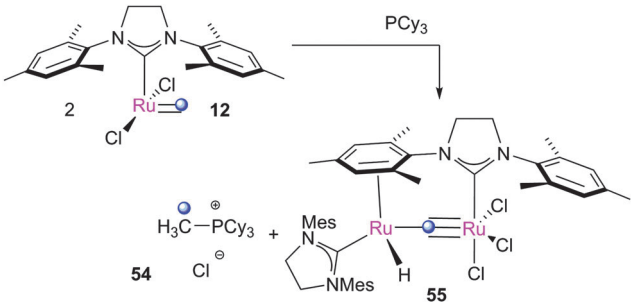

Scheme 25 Decomposition of methylidene complex **53**.

during which the phosphine dissociates and reacts with the alkylidene moiety, forming the phosphine ylide species **54** and dinuclear ruthenium species **55** (Scheme 25).[137,138]

Although the inorganic products of the decomposition of first generation **52** are still unknown, a bimetallic hydride species was isolated from decomposition of **G2**-derived **53**. The proposed mechanism for this reaction goes *via* dissociation of a phosphine, which reacts with the alkylidene, forming phosphonium ylide $Cy_3P{=}CH_2$. The postulated 12e$^-$ ruthenium product can then co-ordinate the mesityl ring of another molecule of **12**, eventually leading to hydride complex **55** after HCl removal by $Cy_3P{=}CH_2$ liberated previously. **55** was shown to be active for the isomerisation of allylbenzene, but Fogg *et al.* later cast doubt on whether the activity of this species can account for all of the observed isomerisation in metathesis reactions.[139] Different behaviour occurs in the presence of ethene (1 atm.), where **12** dimerises to form a chloride bridged cyclometallated species. Grubbs *et al.* screened the stability of a range of methylidene complexes, recording decomposition rates that were highly dependent on the ligand structure (Table 5). Methylidene complexes are also known to be sensitive

Table 5 Decomposition rates of methylidene complexes

Entry		$t_{1/2}$ (min)	k_{decomp} (s^{-1})	Products
1	Cy_3P, Cl, Ru=, Cl, PCy_3	40	0.016	[Cy_3PMe][Cl] (82%)
2	Cy_3P, Br, Ru=, Br, PCy_3	35	0.018	[Cy_3PMe][Br] (85%)
3	SIMes, Cl, Ru=, Cl, PCy_3	340	0.0021	[Cy_3PMe][Cl] (46%)
4	SIMes, Br, Ru=, Br, PCy_3	315	0.0024	[Cy_3PMe][Br]
5	SIPr, Cl, Ru=, Cl, PCy_3	60	0.011	[Cy_3PMe][Cl], IPr·HCl

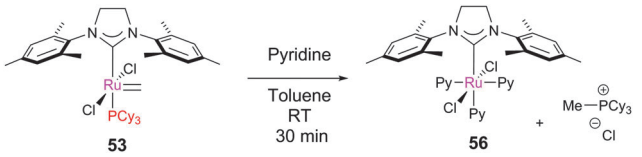

Scheme 26 Decomposition of **53** by reaction with pyridine.

to pyridine; for example, **53** reacts rapidly to form tris(pyridine) complex **56** (Scheme 26).[138]

Deactivation by substrates

Methylidene complexes are not the only vectors for decomposition: reactions with certain substrates can lead to unwanted side reactions of the catalyst.

Cyclopropenyl substrates

When substrates such as Feist ester **57** are employed, **G1** and **G2** decompose to ruthenium carbide complexes **58** and **59**, respectively. The proposed mechanism involves the formation of species **60** or **61** which rearranges, eliminating dimethyl fumarate and the carbide complex **58** and **59** (Scheme 27).[140] Notably, protonation of these species with $[H(OEt_2)_2][B(C_6F_5)]$ leads to Piers-type rapidly-initiating catalysts.[17] $[RuCl_2(PPh_3)_2(CHPh)]$ reacts with the ester to yield only the intermediate carbene.

Electron-rich alkenes

Reactions with vinyl halides have been reported to lead to decomposition in some cases, driven by the stability of the product Fischer-type carbenes.[141] Indeed, these are often used as a catalyst quench or for the determination of initiation rate.

Grubbs *et al.* prepared a series of Fischer carbene complexes *via* the metathesis of vinyl ethers (Scheme 28).[71] The product complexes were found to be much less active than the parent benzylidene species, requiring high temperatures to achieve turnover. In addition, thermolysis of these species leads to ruthenium hydride species (such as **62** and **63**) which may isomerise substrate and product alkenes.[139,142–146]

The reaction of **Piers2** with 1,1-dichloroethene leads to the halide bridged complex **64** (Scheme 29).[147] In addition, catalytically-inactive species **58**, **59**, **65** and **66** have been obtained from the reaction of vinyl halides and vinyl esters

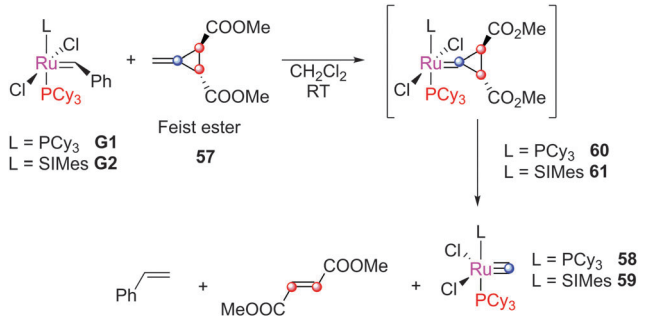

Scheme 27 Decomposition of alkene metathesis pre-catalysts *via* reaction with cyclopropenyl substrates.

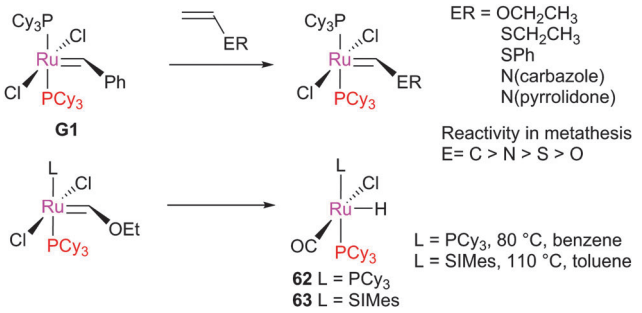

Scheme 28 Metathesis of electron-rich alkenes.

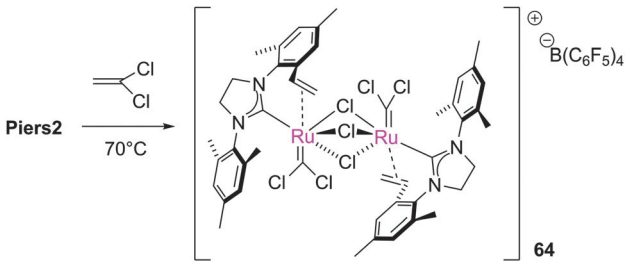

Scheme 29 Reaction of 1,1-dichloroethene with **Piers2**.

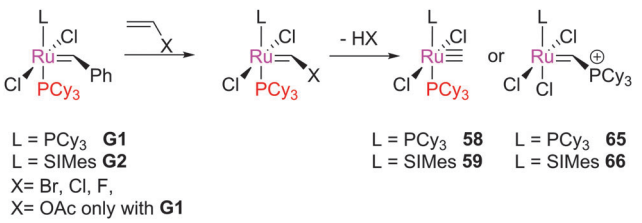

Scheme 30 Metathesis of electron-rich alkenes.

with metathesis pre-catalysts (Scheme 30).[148–150] In some cases the metathesis of vinyl halides can be successful. Stoltz reported the synthesis of elatol, *via* a spirocyclic intermediate bearing a vinyl chloride.[72,151] Notably, the methodology used avoids the formation of an α-chloro alkylidene intermediate. Dorta and co-workers conducted a rational study to elucidate how RCM to form such halogenated alkenes might be achieved, by analysing the results of the RCM of a series of vinyl bromides (Scheme 31).[152] However, only diene **67**, with a phenyl substituent *cis* to the bromide, achieved complete conversion to the product. In the Dorta example, formation of an α-haloalkylidene might also be avoided, if reaction with the alternative terminus is faster.

Acrylonitrile is traditionally a very difficult substrate, due to the formation of inactive complexes such as **68**. The use of phosphine-free catalysts such as **G2-py** can overcome this issue, by precluding the capture of $14e^-$ alkylidenes by phosphine.[13]

Ligand C–H activation

When the *N*-aryl substituents on the imidazolium ring can rotate to interact with the ruthenium centre, C–H activation can occur. There are two possible types of C–H insertion: to

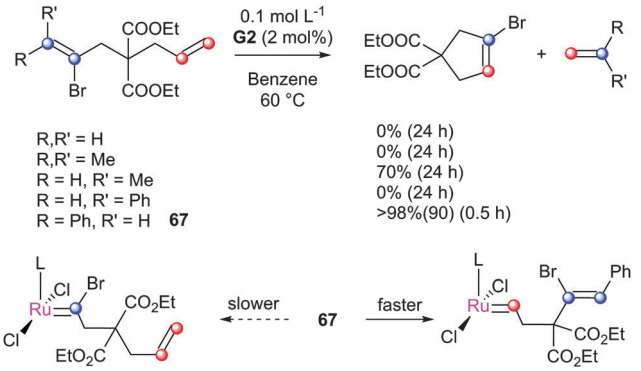

Scheme 31 Metathesis of vinyl bromide substrates.

form ruthenium metallacycles, or insertion of the alkylidene moiety. Grubbs reported the spontaneous double C–H activation of **69** to form **70** (Scheme 32).[153] This interesting rearrangement has been computationally studied by Cavallo and Suresh;[154–156] the *N*-phenyl substituent, due to the relatively low barriers to rotation, can be *ortho*-metallated, obtaining intermediate **71**, which immediately rearranges to complex **72**. This complex can insert into the C–H on the other *N*-phenyl moiety, achieving the final product **70**. Bulkier *N*-aryl substituents impede this rotation, precluding the C–H activation process.

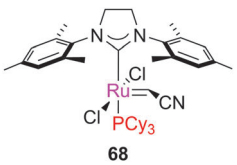

68

A different C–H insertion process can occur *via* the alkylidene moiety. This decomposition can occur, for example, in the presence of oxygen. Blechert proposed that **73** can undergo

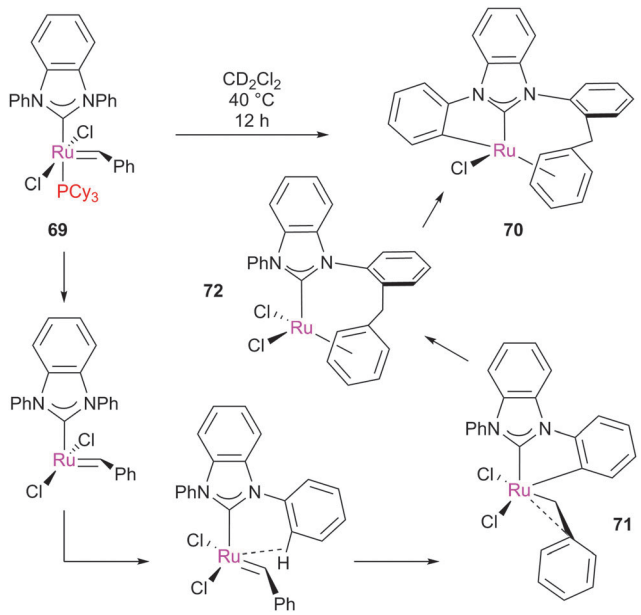

Scheme 32 C–H insertion in complex **69**.

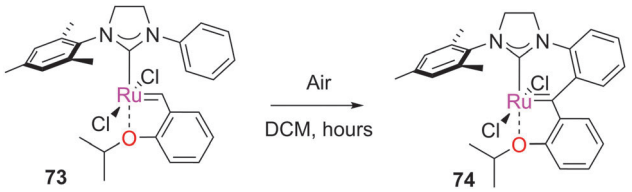

Scheme 33 C–H insertion in a Hoveyda-type complex.

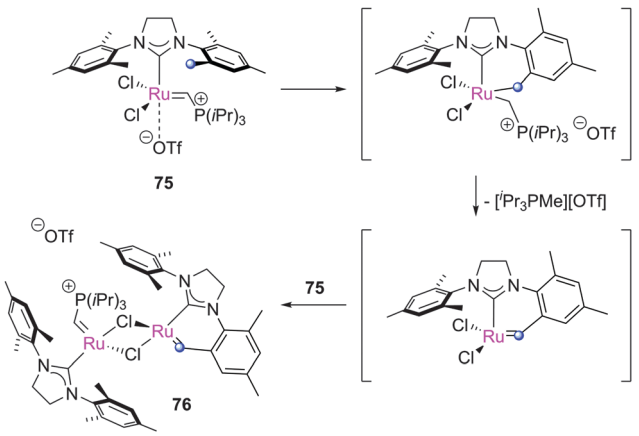

Scheme 34 Decomposition of **75**.

intramolecular C–H insertion into the alkylidene moiety through a pericyclic rearrangement of the aryl substituent to form the carbene arene complex **74** (Scheme 33).[157] C–H insertion can also occur if the catalyst is not thermally stable in solution; for example, Piers reported that pre-catalyst **75**, after two days at room temperature, dimerised to form complex **76** (Scheme 34).

In certain cases, cyclometallation of the ligand allows the generation of new pre-catalysts with new reactivity. For example, **45** underwent reaction with $^{t}BuCO_2Ag$, followed by insertion of the ruthenium centre into a C–H bond on the *N*-adamantyl substituent to form complex **44** (Scheme 21, above).[128,158] This complex was revealed to be *Z*-selective in CM reactions. This methodology has been studied in detail with several pre-catalyst motifs, revealing that the synthetic route to **44** is specific to this NHC (Scheme 35). Increasing the bulkiness of the *N*-aryl substituent or changing the adamantyl substituent to an aromatic moiety caused decomposition.[159]

π-Acids

π-Acids such as CO react with pre-catalysts, forming metathesis-inactive decomposition products. First reported by Diver, exposing **G2** or methylidene **53** to 1 atm. CO at room temperature results in the rapid rearrangement of the carbene moiety, which inserts into the *N*-aryl substituent *via* a Buchner-type mechanism, leading to complexes such as **77** (Scheme 36).[160] Similar reactivity was demonstrated with isocyanides and with different second generation pre-catalysts.[161] An interesting application is the use of $CNCH_2CO_2K$ as a catalyst scavenger, which generates complexes such as **78** that can be easily removed from the reaction mixture.[162] The mechanism of this

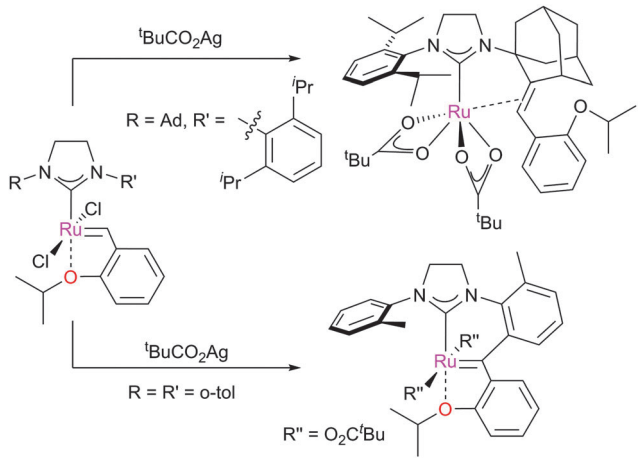

Scheme 35 Decomposition of pre-catalysts promoted by $^{t}BuCO_2Ag$.

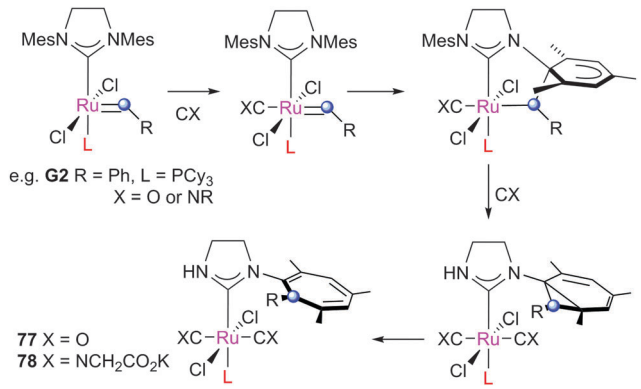

Scheme 36 π-acid promoted decomposition of metathesis catalysts.

reaction has been investigated computationally by Cavallo, who suggested that it proceeds *via* reaction of the *ipso* carbon of the *N*-aryl substituent with the carbene, promoted by the π-acidity of the ligand *trans* to the alkylidene.[163]

Another decomposition route involving CO was reported by Grubbs with cyclometallated complex **44**. It was found that at −78 °C in the presence of excess CO, the co-ordination of CO to the ruthenium centre promotes the C–H insertion of the *N*-adamantyl substituent into the carbene moiety, achieving complex **79** (Scheme 37).[159] This C–H activation is due to the ligand substitution by the π-acidic CO ligands, which decreases the ability of the metal centre to stabilise the alkylidene by back-bonding. This lack of stabilisation is presumably relieved by the C–H *N*-adamantyl substituent in the alkylidene forming inactive complex **79**.

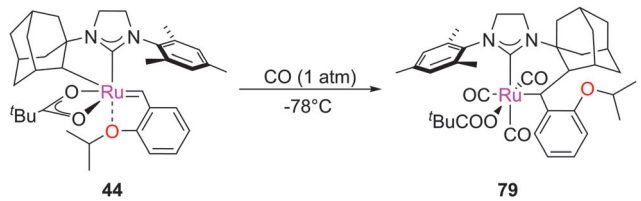

Scheme 37 Decomposition of complex **44**.

Alcoholysis

The alcoholysis of metathesis pre-catalysts in the presence of base has been reported to lead to (typically hydride) decomposition products, which are interesting not only as decomposition products but as catalysts in tandem metathesis/hydrogenation or metathesis/isomerisation processes.[164,165] Mol *et al.* carried out a number of studies, stirring complexes such as **G1** and **G2** in methanol in the presence of a base. This caused decomposition to hydridocarbonyl complexes **62** and **63** respectively (Scheme 38).[144–146] A mechanism for the alcoholysis reaction was tentatively suggested by Mol, which was somewhat supported by labelling experiments. Notably, the use of alcohols such as ethanol in this process means that a carbon–carbon bond breaking process must occur during the reaction; ^{13}C labelling experiments confirmed that the ethanol was the source of the CO ligand. This mechanism was recently studied by Percy, Hillier and Tuttle using DFT calculations (Scheme 39).[142,145]

Different behaviour was observed with indenylidene species $\mathbf{M_{10}}$ and $\mathbf{M_{11}}$, while $\mathbf{M_1}$ behaved as **G1**. In basic alcohol solution, $\mathbf{M_{10}}$ (a starting material for most indenylidene pre-catalysts) undergoes reaction to form an η^5-indenyl species [RuCl(η^5-3-phenylindenyl)(PPh_3)$_2$] **80** (Scheme 40).[166] This new complex has been found to be highly active in a number of transformations, from alcohol racemisation to carboxylic acid reduction.[167] Analogous complex $\mathbf{M_{11}}$ undergoes a similar reaction, but reacts further to form hydride species **81**.[168]

A subsequent detailed study established that PCy_3-bearing complexes such as **G1**, $\mathbf{M_1}$, and **G1**-derived **52** decomposed in primary alcohols to yield hydridocarbonyl complex **62**, and in secondary alcohols to yield hydrogenohydride species **82** (Scheme 41).[169] Notably, the synthesis of the latter species requires the use of dihydrogen in all other reports. The different behaviour of complexes bearing different phosphine ligands was rationalised

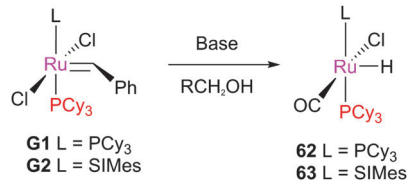

Scheme 38 Alcoholysis of benzylidene complexes.

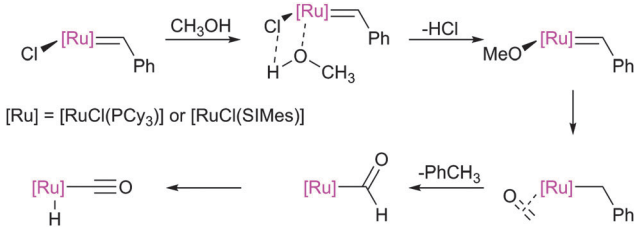

Scheme 39 Proposed mechanism for the decomposition of benzylidene complexes by alcoholysis.

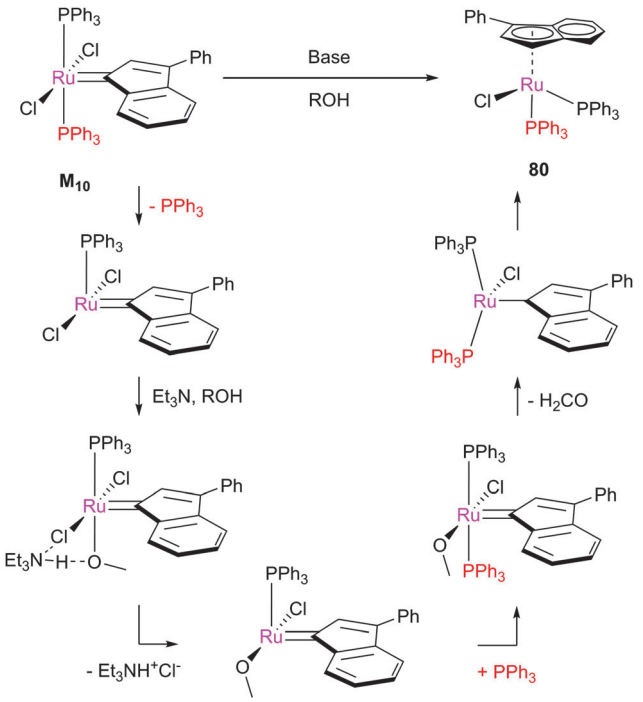

Scheme 40 Alcoholysis of $\mathbf{M_{10}}$.

by DFT studies of the potential energy surfaces for formation of the η^5-complexes bearing triphenylphosphine, tricyclohexylphosphine, and iso-butylphoban ligands.

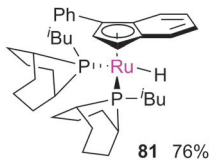

Treating **G1** and **G2** with benzyl alcohol, and a base such as triethylamine, does not form the expected hydridocarbonyl complexes, but a different species where the phenyl is directly bonded to the ruthenium centre (Scheme 42).[145] The SIMes-bearing product was also obtained when **G2** was exposed to oxygen, although other side products, such as **83**, have also been attributed to the reaction of **G2** with oxygen.[170]

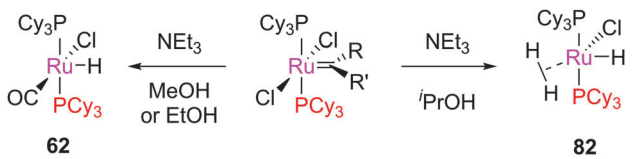

Scheme 41 Decomposition of tricyclohexylphosphine-containing complexes in primary *versus* secondary alcohols.

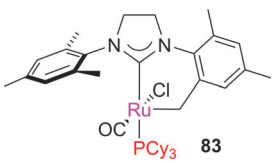

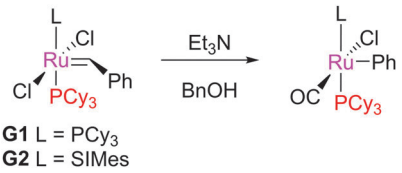

Scheme 42 Decomposition of benzylidene complexes in benzyl alcohol.

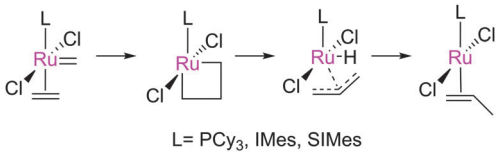

Scheme 43 Decomposition *via* hydride abstraction in MCBs.

Other routes

Van Rensburg and co-workers have studied the decomposition of ruthenium metathesis catalysts *via* hydride abstraction in the MCB to yield an η^3-allyl complex (Scheme 43).[171,172] The observed decomposition products (experimentally) were in agreement with the calculated decomposition route.[142]

Conclusions and outlook

Recent research in the field of alkene metathesis, most of it within the last 15 years or so, has improved our understanding of mechanistic details of alkene metathesis reactions. The initiation of a variety of pre-catalysts, key steps during the catalytic cycle, and the decomposition of metathesis (pre-)catalysts have all been explored by a range of researchers, using a number of techniques such as NMR spectroscopy, DFT studies, and mass spectrometry. Highlights include: a detailed understanding of pre-catalyst initiation, including how various structural features influence the rate of this process and therefore the rate of delivery of the active catalyst into solution; probing of key steps of the mechanism such as the formation and breakdown of MCBs and how these depend on catalyst and substrate structure; and the characterisation and redeployment of interesting decomposition products. These studies have helped to guide the development of future catalysts and reactions. It is now well-accepted that there is no single 'best' pre-catalyst; mechanistic details available in the literature allow the end users of metathesis technology to select an appropriate balance of initiation rate and thermal stability, based on their specific application. Future work in the area will undoubtedly continue to yield new catalysts with new reactivity profiles, as well as further elegant uses of metathesis techniques in synthetic and materials chemistry.

Acknowledgements

Work on metathesis chemistry within our research group has received funding from a number of sources, to whom we are very grateful. These include: the EPSRC, the ERC (*via* Advanced Investigator Grant 'FUNCAT' to SPN), the EC (*via* FP7 project 'EUMET')

and Umicore (for gifts of materials). SPN is a Royal Society Wolfson Research Merit Award holder.

Notes and references

1 Y. Chauvin, *Angew. Chem., Int. Ed.*, 2006, **45**, 3740–3747.
2 R. H. Grubbs, *Angew. Chem., Int. Ed.*, 2006, **45**, 3760–3765.
3 R. R. Schrock, *Angew. Chem., Int. Ed.*, 2006, **45**, 3748–3759.
4 D. Astruc, *New J. Chem.*, 2005, **29**, 42–56.
5 G. C. Lloyd-Jones, in *The Investigation of Organic Reactions and Their Mechanisms*, ed. H. Maskill, Wiley Blackwell, Oxford, 2006, pp. 343–352.
6 C. Samojlowicz, M. Bieniek and K. Grela, *Chem. Rev.*, 2009, **109**, 3708–3742.
7 G. C. Vougioukalakis and R. H. Grubbs, *Chem. Rev.*, 2009, **110**, 1746–1787.
8 S. Díez-González, N. Marion and S. P. Nolan, *Chem. Rev.*, 2009, **109**, 3612–3676.
9 P. J.-L. Hérisson and Y. Chauvin, *Makromol. Chem.*, 1970, **141**, 161–176.
10 F. Boeda, H. Clavier and S. P. Nolan, *Chem. Commun.*, 2008, 2726–2740.
11 P. Schwab, M. B. France, J. W. Ziller and R. H. Grubbs, *Angew. Chem., Int. Ed. Engl.*, 1995, **34**, 2039–2041.
12 M. Scholl, S. Ding, C. W. Lee and R. H. Grubbs, *Org. Lett.*, 1999, **1**, 953–956.
13 J. A. Love, J. P. Morgan, T. M. Trnka and R. H. Grubbs, *Angew. Chem., Int. Ed.*, 2002, **41**, 4035–4037.
14 S. B. Garber, J. S. Kingsbury, B. L. Gray and A. H. Hoveyda, *J. Am. Chem. Soc.*, 2000, **122**, 8168–8179.
15 J. S. Kingsbury, J. P. A. Harrity, P. J. Bonitatebus and A. H. Hoveyda, *J. Am. Chem. Soc.*, 1999, **121**, 791–799.
16 A. Michrowska, R. Bujok, S. Harutyunyan, V. Sashuk, G. Dolgonos and K. Grela, *J. Am. Chem. Soc.*, 2004, **126**, 9318–9325.
17 P. E. Romero, W. E. Piers and R. McDonald, *Angew. Chem., Int. Ed.*, 2004, **43**, 6161–6165.
18 S. R. Dubberley, P. E. Romero, W. E. Piers, R. McDonald and M. Parvez, *Inorg. Chim. Acta*, 2006, **359**, 2658–2664.
19 J. Huang, E. D. Stevens, S. P. Nolan and J. L. Petersen, *J. Am. Chem. Soc.*, 1999, **121**, 2674–2678.
20 R. Credendino, A. Poater, F. Ragone and L. Cavallo, *Catal. Sci. Technol.*, 2011, **1**, 1287–1297.
21 J. I. du Toit, C. G. C. E. van Sittert and H. C. M. Vosloo, *J. Organomet. Chem.*, 2013, **738**, 76–91.
22 E. L. Dias, S. T. Nguyen and R. H. Grubbs, *J. Am. Chem. Soc.*, 1997, **119**, 3887–3897.
23 M. S. Sanford, M. Ulman and R. H. Grubbs, *J. Am. Chem. Soc.*, 2001, **123**, 749–750.
24 D. J. Nelson and S. P. Nolan, *Chem. Soc. Rev.*, 2013, **42**, 6723–6753.
25 M. S. Sanford, J. A. Love and R. H. Grubbs, *J. Am. Chem. Soc.*, 2001, **123**, 6543–6554.
26 J. A. Love, M. S. Sanford, M. W. Day and R. H. Grubbs, *J. Am. Chem. Soc.*, 2003, **125**, 10103–10109.
27 I. W. Ashworth, D. J. Nelson and J. M. Percy, *Dalton Trans.*, 2013, **42**, 4110–4113.
28 C. Samojłowicz, M. Bieniek, A. Pazio, A. Makal, K. Woźniak, A. Poater, L. Cavallo, J. Wójcik, K. Zdanowski and K. Grela, *Chem. – Eur. J.*, 2011, **17**, 12981–12993.
29 C. Samojlowicz, M. Bieniek, A. Zarecki, R. Kadyrov and K. Grela, *Chem. Commun.*, 2008, 6282–6284.
30 K. Getty, M. U. Delgado-Jaime and P. Kennepohl, *J. Am. Chem. Soc.*, 2007, **129**, 15774–15776.
31 Y. Zhao and D. G. Truhlar, *Org. Lett.*, 2007, **9**, 1967–1970.
32 I. C. Stewart, D. Benitez, D. J. O'Leary, E. Tkatchouk, M. W. Day, W. A. Goddard and R. H. Grubbs, *J. Am. Chem. Soc.*, 2009, **131**, 1931–1938.
33 Y. Minenkov, G. Occhipinti, W. Heyndrickx and V. R. Jensen, *Eur. J. Inorg. Chem.*, 2012, 1507–1516.
34 H.-C. Yang, Y.-C. Huang, Y.-K. Lan, T.-Y. Luh, Y. Zhao and D. G. Truhlar, *Organometallics*, 2011, **30**, 4196–4200.
35 C. A. Urbina-Blanco, A. Poater, T. Lebl, S. Manzini, A. M. Z. Slawin, L. Cavallo and S. P. Nolan, *J. Am. Chem. Soc.*, 2013, **135**, 7073–7079.
36 G. C. Vougioukalakis and R. H. Grubbs, *Chem. – Eur. J.*, 2008, **14**, 7545–7556.
37 T. Vorfalt, K. J. Wannowius and H. Plenio, *Angew. Chem., Int. Ed.*, 2010, **49**, 5533–5536.
38 I. W. Ashworth, I. H. Hillier, D. J. Nelson, J. M. Percy and M. A. Vincent, *Chem. Commun.*, 2011, **47**, 5428–5430.
39 V. Thiel, M. Hendann, K.-J. Wannowius and H. Plenio, *J. Am. Chem. Soc.*, 2011, **134**, 1104–1114.
40 F. Nuñez-Zarur, X. Solans-Monfort, L. Rodríguez-Santiago and M. Sodupe, *Organometallics*, 2012, **31**, 4203–4215.
41 D. J. Nelson and J. M. Percy, *Dalton Trans.*, 2014, **43**, 4674–4679.
42 D. J. Nelson, P. Queval, M. Rouen, M. Magrez, L. Toupet, F. Caijo, E. Borré, I. Laurent, C. Crévisy, O. Baslé, M. Mauduit and J. M. Percy, *ACS Catal.*, 2013, **3**, 259–264.
43 I. W. Ashworth, I. H. Hillier, D. J. Nelson, J. M. Percy and M. A. Vincent, *ACS Catal.*, 2013, **3**, 1929–1939.
44 M. Barbasiewicz, A. Szadkowska, A. Makal, K. Jarzembska, K. Woźniak and K. Grela, *Chem. – Eur. J.*, 2008, **14**, 9330–9337.
45 M. Barbasiewicz, K. Grudzień and M. Malinska, *Organometallics*, 2012, **31**, 3171–3177.
46 P. E. Romero and W. E. Piers, *J. Am. Chem. Soc.*, 2005, **127**, 5032–5033.
47 P. E. Romero and W. E. Piers, *J. Am. Chem. Soc.*, 2007, **129**, 1698–1704.
48 E. F. van der Eide, P. E. Romero and W. E. Piers, *J. Am. Chem. Soc.*, 2008, **130**, 4485–4491.
49 E. M. Leitao, E. F. v. d. Eide, P. E. Romero, W. E. Piers and R. McDonald, *J. Am. Chem. Soc.*, 2010, **132**, 2784–2794.
50 E. F. van der Eide and W. E. Piers, *Nat. Chem.*, 2010, **2**, 571–576.
51 A. G. Wenzel and R. H. Grubbs, *J. Am. Chem. Soc.*, 2006, **128**, 16048–16049.
52 A. G. Wenzel, G. Blake, D. G. VanderVelde and R. H. Grubbs, *J. Am. Chem. Soc.*, 2011, **133**, 6429–6439.
53 B. K. Keitz and R. H. Grubbs, *J. Am. Chem. Soc.*, 2011, **133**, 16277–16284.
54 A. K. Chatterjee, T.-L. Choi, D. P. Sanders and R. H. Grubbs, *J. Am. Chem. Soc.*, 2003, **125**, 11360–11370.
55 C. A. Tolman, *Chem. Rev.*, 1977, **77**, 313–348.
56 X. Bantreil, T. E. Schmid, R. A. M. Randall, A. M. Z. Slawin and C. S. J. Cazin, *Chem. Commun.*, 2010, **46**, 7115–7117.
57 X. Bantreil, A. Poater, C. A. Urbina-Blanco, Y. D. Bidal, L. Falivene, R. A. M. Randall, L. Cavallo, A. M. Z. Slawin and C. S. J. Cazin, *Organometallics*, 2012, **31**, 7415–7426.
58 T. E. Schmid, X. Bantreil, C. A. Citadelle, A. M. Z. Slawin and C. S. J. Cazin, *Chem. Commun.*, 2011, **47**, 7060–7062.
59 C. A. Urbina-Blanco, X. Bantreil, J. Wappel, T. E. Schmid, A. M. Z. Slawin, C. Slugovc and C. S. J. Cazin, *Organometallics*, 2013, **32**, 6240–6247.
60 S. Monsaert, A. Lozano Vila, R. Drozdzak, P. Van Der Voort and F. Verpoort, *Chem. Soc. Rev.*, 2009, **38**, 3360–3372.
61 Y. Vidavsky, A. Anaby and N. G. Lemcoff, *Dalton Trans.*, 2012, **41**, 32–43.
62 M. Barbasiewicz, A. Szadkowska, R. Bujok and K. Grela, *Organometallics*, 2006, **25**, 3599–3604.
63 A. Poater, F. Ragone, A. Correa, A. Szadkowska, M. Barbasiewicz, K. Grela and L. Cavallo, *Chem. – Eur. J.*, 2010, **16**, 14354–14364.
64 E. Tzur, A. Szadkowska, A. Ben-Asuly, A. Makal, I. Goldberg, K. Woźniak, K. Grela and N. G. Lemcoff, *Chem. – Eur. J.*, 2010, **16**, 8726–8737.
65 M. Barbasiewicz, M. Michalak and K. Grela, *Chem. – Eur. J.*, 2012, **18**, 14237–14241.
66 K. Grudzień, K. Żukowska, M. Malińska, K. Woźniak and M. Barbasiewicz, *Chem. – Eur. J.*, 2014, **20**, 2819–2828.
67 K. Żukowska, A. Szadkowska, B. Trzaskowski, A. Pazio, Ł. Pączek, K. Woźniak and K. Grela, *Organometallics*, 2013, **32**, 2192–2198.
68 B. Trzaskowski and K. Grela, *Organometallics*, 2013, **32**, 3625–3630.
69 T. Weskamp, W. C. Schattenmann, M. Spiegler and W. A. Herrmann, *Angew. Chem., Int. Ed.*, 1998, **37**, 2490–2493.
70 M. Scholl, T. M. Trnka, J. P. Morgan and R. H. Grubbs, *Tetrahedron Lett.*, 1999, **40**, 2247–2250.
71 J. Louie and R. H. Grubbs, *Organometallics*, 2002, **21**, 2153–2164.
72 D. E. White, I. C. Stewart, R. H. Grubbs and B. M. Stoltz, *J. Am. Chem. Soc.*, 2007, **130**, 810–811.
73 M. Bieniek, A. Michrowska, D. L. Usanov and K. Grela, *Chem. – Eur. J.*, 2008, **14**, 806–818.

74 S. Monfette and D. E. Fogg, *Chem. Rev.*, 2009, **109**, 3783–3816.
75 D. J. Nelson, I. W. Ashworth, I. H. Hillier, S. H. Kyne, S. Pandian, J. A. Parkinson, J. M. Percy, G. Rinaudo and M. A. Vincent, *Chem. – Eur. J.*, 2011, **17**, 13087–13094.
76 T. Ritter, A. Hejl, A. G. Wenzel, T. W. Funk and R. H. Grubbs, *Organometallics*, 2006, **25**, 5740–5745.
77 D. Bourgeois, A. Pancrazi, L. Ricard and J. Prunet, *Angew. Chem., Int. Ed.*, 2000, **39**, 725–728.
78 A. Gradillas and J. P. Castells, *Angew. Chem., Int. Ed.*, 2006, **45**, 6086–6101.
79 L. Cavallo, *J. Am. Chem. Soc.*, 2002, **124**, 8965–8973.
80 B. F. Straub, *Angew. Chem., Int. Ed.*, 2005, **44**, 5974–5978.
81 B. F. Straub, *Adv. Synth. Catal.*, 2007, **349**, 204–214.
82 I. Fernández, N. Lugan and G. Lavigne, *Organometallics*, 2012, **31**, 1155–1160.
83 M. Sussner and H. Plenio, *Chem. Commun.*, 2005, 5417–5419.
84 S. Leuthäußer, V. Schmidts, C. M. Thiele and H. Plenio, *Chem. – Eur. J.*, 2008, **14**, 5465–5481.
85 R. Credendino, L. Falivene and L. Cavallo, *J. Am. Chem. Soc.*, 2012, **134**, 8127–8135.
86 J.-H. Sohn, K. H. Kim, H.-Y. Lee, Z. S. No and H. Ihee, *J. Am. Chem. Soc.*, 2008, **130**, 16506–16507.
87 K. H. Kim, T. Ok, K. Lee, H.-S. Lee, K. T. Chang, H. Ihee and J.-H. Sohn, *J. Am. Chem. Soc.*, 2010, **132**, 12027–12033.
88 L. Benhamou, E. Chardon, G. Lavigne, S. Bellemin-Laponnaz and V. César, *Chem. Rev.*, 2011, **111**, 2705–2733.
89 H. Clavier and S. P. Nolan, *Chem. Commun.*, 2010, **46**, 841–861.
90 F. Ragone, A. Poater and L. Cavallo, *J. Am. Chem. Soc.*, 2010, **132**, 4249–4258.
91 A. Poater, B. Cosenza, A. Correa, S. Giudice, F. Ragone, V. Scarano and L. Cavallo, *Eur. J. Inorg. Chem.*, 2009, 1759–1766.
92 T. Dröge and F. Glorius, *Angew. Chem., Int. Ed.*, 2010, **49**, 6940–6952.
93 R. M. Thomas, B. K. Keitz, T. M. Champagne and R. H. Grubbs, *J. Am. Chem. Soc.*, 2011, **133**, 7490–7496.
94 S. Kavitake, M. K. Samantaray, R. Dehn, S. Deuerlein, M. Limbach, J. A. Schachner, E. Jeanneau, C. Coperet and C. Thieuleux, *Dalton Trans.*, 2011, **40**, 12443–12446.
95 A. J. Kirby, *Adv. Phys. Org. Chem.*, 1980, **17**, 183–278.
96 L. Mandolini, *Adv. Phys. Org. Chem.*, 1986, **22**, 1–111.
97 J. C. Conrad, M. D. Eelman, J. A. D. Silva, S. Monfette, H. H. Parnas, J. L. Snelgrove and D. E. Fogg, *J. Am. Chem. Soc.*, 2007, **129**, 1024–1025.
98 C. Galli and L. Mandolini, *Eur. J. Org. Chem.*, 2000, 3117–3125.
99 L. Mitchell, J. A. Parkinson, J. M. Percy and K. Singh, *J. Org. Chem.*, 2008, **73**, 2389–2395.
100 I. W. Ashworth, D. Carboni, I. H. Hillier, D. J. Nelson, J. M. Percy, G. Rinaudo and M. A. Vincent, *Chem. Commun.*, 2010, **46**, 7145–7147.
101 H. A. Skinner and G. Pilcher, *Q. Rev., Chem. Soc.*, 1963, **17**, 264–288.
102 C. Hinderling, C. Adlhart and P. Chen, *Angew. Chem., Int. Ed.*, 1998, **37**, 2685–2689.
103 C. Adlhart and P. Chen, *Helv. Chim. Acta*, 2000, **83**, 2192–2196.
104 C. Adlhart, C. Hinderling, H. Baumann and P. Chen, *J. Am. Chem. Soc.*, 2000, **122**, 8204–8214.
105 C. Adlhart, M. A. O. Volland, P. Hofmann and P. Chen, *Helv. Chim. Acta*, 2000, **83**, 3306–3311.
106 S. Torker, D. Merki and P. Chen, *J. Am. Chem. Soc.*, 2008, **130**, 4808–4814.
107 H. Wang and J. r. O. Metzger, *Organometallics*, 2008, **27**, 2761–2766.
108 H.-Y. Wang, W.-L. Yim, T. Kluner and J. O. Metzger, *Chem. – Eur. J.*, 2009, **15**, 10948–10959.
109 H.-Y. Wang, W.-L. Yim, Y.-L. Guo and J. O. Metzger, *Organometallics*, 2012, **31**, 1627–1634.
110 C. E. Webster, *J. Am. Chem. Soc.*, 2007, **129**, 7490–7491.
111 C. N. Rowley, E. F. van der Eide, W. E. Piers and T. K. Woo, *Organometallics*, 2008, **27**, 6043–6045.
112 I. C. Stewart, B. K. Keitz, K. M. Kuhn, R. M. Thomas and R. H. Grubbs, *J. Am. Chem. Soc.*, 2010, **132**, 8534–8535.
113 M. Ulman and R. H. Grubbs, *Organometallics*, 1998, **17**, 2484–2489.
114 D. R. Lane, C. M. Beavers, M. M. Olmstead and N. E. Schore, *Organometallics*, 2009, **28**, 6789–6797.
115 D. J. Nelson, D. Carboni, I. W. Ashworth and J. M. Percy, *J. Org. Chem.*, 2011, **76**, 8386–8393.
116 D. R. Anderson, D. D. Hickstein, D. J. O'Leary and R. H. Grubbs, *J. Am. Chem. Soc.*, 2006, **128**, 8386–8387.
117 J. A. Tallarico, P. J. Bonitatebus and M. L. Snapper, *J. Am. Chem. Soc.*, 1997, **119**, 7157–7158.
118 D. Anderson, D. O'Leary and R. Grubbs, *Chem. – Eur. J.*, 2008, **14**, 7536–7544.
119 T. Vorfalt, K. J. Wannowius, V. Thiel and H. Plenio, *Chem. – Eur. J.*, 2010, **16**, 12312–12315.
120 F. Núñez-Zarur, X. Solans-Monfort, R. Pleixats, L. Rodríguez-Santiago and M. Sodupe, *Chem. – Eur. J.*, 2013, **19**, 14553–14565.
121 C. Luján and S. P. Nolan, *J. Organomet. Chem.*, 2011, **696**, 3935–3938.
122 C. Luján and S. P. Nolan, *Catal. Sci. Technol.*, 2012, **2**, 1027–1032.
123 S. Shahane, C. Bruneau and C. Fischmeister, *ChemCatChem*, 2013, **5**, 3436–3459.
124 A. Fürstner, *Science*, 2013, **341**, 1229713.
125 M. M. Flook, A. J. Jiang, R. R. Schrock, P. Müller and A. H. Hoveyda, *J. Am. Chem. Soc.*, 2009, **131**, 7962–7963.
126 I. Ibrahem, M. Yu, R. R. Schrock and A. H. Hoveyda, *J. Am. Chem. Soc.*, 2009, **131**, 3844–3845.
127 K. Endo and R. H. Grubbs, *J. Am. Chem. Soc.*, 2011, **133**, 8525–8527.
128 B. K. Keitz, K. Endo, P. R. Patel, M. B. Herbert and R. H. Grubbs, *J. Am. Chem. Soc.*, 2011, **134**, 693–699.
129 P. Liu, X. Xu, X. Dong, B. K. Keitz, M. B. Herbert, R. H. Grubbs and K. N. Houk, *J. Am. Chem. Soc.*, 2012, **134**, 1464–1467.
130 D. Benitez, E. Tkatchouk and W. A. Goddard III, *Chem. Commun.*, 2008, 6194–6196.
131 Y. Dang, Z.-X. Wang and X. Wang, *Organometallics*, 2012, **31**, 7222–7234.
132 X. Solans-Monfort, R. Pleixats and M. Sodupe, *Chem. – Eur. J.*, 2010, **16**, 7331–7343.
133 Y. Dang, Z.-X. Wang and X. Wang, *Organometallics*, 2012, **31**, 8654–8657.
134 G. Occhipinti, F. R. Hansen, K. W. Törnroos and V. R. Jensen, *J. Am. Chem. Soc.*, 2013, **135**, 3331–3334.
135 S. Torker, R. K. M. Khan and A. H. Hoveyda, *J. Am. Chem. Soc.*, 2014, **136**, 3439–3455.
136 R. K. M. Khan, S. Torker and A. H. Hoveyda, *J. Am. Chem. Soc.*, 2013, **135**, 10258–10261.
137 S. H. Hong, M. W. Day and R. H. Grubbs, *J. Am. Chem. Soc.*, 2004, **126**, 7414–7415.
138 S. H. Hong, A. G. Wenzel, T. T. Salguero, M. W. Day and R. H. Grubbs, *J. Am. Chem. Soc.*, 2007, **129**, 7961–7968.
139 C. S. Higman, L. Plais and D. E. Fogg, *ChemCatChem*, 2013, **5**, 3548–3551.
140 R. G. Carlson, M. A. Gile, J. A. Heppert, M. H. Mason, D. R. Powell, D. V. Velde and J. M. Vilain, *J. Am. Chem. Soc.*, 2002, **124**, 1580–1581.
141 Y. Minenkov, G. Occhipinti and V. R. Jensen, *Organometallics*, 2013, **32**, 2099–2111.
142 I. W. Ashworth, I. H. Hillier, D. J. Nelson, J. M. Percy and M. A. Vincent, *Eur. J. Org. Chem.*, 2012, 5673–5677.
143 A. Young, M. A. Vincent, I. H. Hillier, J. M. Percy and T. Tuttle, *Dalton Trans.*, 2014, **43**, 8493–8498.
144 M. B. Dinger and J. C. Mol, *Eur. J. Inorg. Chem.*, 2003, 2827–2833.
145 M. B. Dinger and J. C. Mol, *Organometallics*, 2003, **22**, 1089–1095.
146 D. Banti and J. C. Mol, *J. Organomet. Chem.*, 2004, **689**, 3113–3116.
147 E. Leitao, S. Dubberley, W. Piers, Q. Wu and R. McDonald, *Chem. – Eur. J.*, 2008, **14**, 11565–11572.
148 M. L. Macnaughtan, M. J. A. Johnson and J. W. Kampf, *J. Am. Chem. Soc.*, 2007, **129**, 7708–7709.
149 M. L. Macnaughtan, J. B. Gary, D. L. Gerlach, M. J. A. Johnson and J. W. Kampf, *Organometallics*, 2009, **28**, 2880–2887.
150 M. L. Macnaughtan, M. J. A. Johnson and J. W. Kampf, *Organometallics*, 2007, **26**, 780–782.
151 D. E. White, I. C. Stewart, B. A. Seashore-Ludlow, R. H. Grubbs and B. M. Stoltz, *Tetrahedron*, 2010, **66**, 4668–4686.
152 M. Gatti, E. Drinkel, L. Wu, I. Pusterla, F. Gaggia and R. Dorta, *J. Am. Chem. Soc.*, 2010, **132**, 15179–15181.
153 S. H. Hong, A. Chlenov, M. W. Day and R. H. Grubbs, *Angew. Chem., Int. Ed.*, 2007, **46**, 5148–5151.
154 A. Poater and L. Cavallo, *J. Mol. Catal. A: Chem.*, 2010, **324**, 75–79.
155 A. Poater, N. Bahri-Laleh and L. Cavallo, *Chem. Commun.*, 2011, **47**, 6674–6676.

156 J. Mathew, N. Koga and C. H. Suresh, *Organometallics*, 2008, **27**, 4666–4670.
157 K. Vehlow, S. Gessler and S. Blechert, *Angew. Chem., Int. Ed.*, 2007, **46**, 8082–8085.
158 B. K. Keitz, K. Endo, M. B. Herbert and R. H. Grubbs, *J. Am. Chem. Soc.*, 2011, **133**, 9686–9688.
159 M. B. Herbert, Y. Lan, B. K. Keitz, P. Liu, K. Endo, M. W. Day, K. N. Houk and R. H. Grubbs, *J. Am. Chem. Soc.*, 2012, **134**, 7861–7866.
160 B. R. Galan, M. Gembicky, P. M. Dominiak, J. B. Keister and S. T. Diver, *J. Am. Chem. Soc.*, 2005, **127**, 15702–15703.
161 B. R. Galan, M. Pitak, M. Gembicky, J. B. Keister and S. T. Diver, *J. Am. Chem. Soc.*, 2009, **131**, 6822–6832.
162 B. R. Galan, K. P. Kalbarczyk, S. Szczepankiewicz, J. B. Keister and S. T. Diver, *Org. Lett.*, 2007, **9**, 1203–1206.
163 A. Poater, F. Ragone, A. Correa and L. Cavallo, *J. Am. Chem. Soc.*, 2009, **131**, 9000–9006.
164 B. Schmidt, *J. Mol. Catal. A: Chem.*, 2006, **254**, 53–57.
165 B. Schmidt, *Eur. J. Org. Chem.*, 2004, 1865–1880.
166 S. Manzini, C. A. Urbina-Blanco, A. Poater, A. M. Z. Slawin, L. Cavallo and S. P. Nolan, *Angew. Chem.*, 2012, **124**, 1066–1069.
167 J. A. Fernández-Salas, S. Manzini and S. P. Nolan, *Adv. Synth. Catal.*, 2014, **356**, 308–312.
168 S. Manzini, D. J. Nelson, T. Lebl, A. Poater, L. Cavallo, A. M. Z. Slawin and S. P. Nolan, *Chem. Commun.*, 2014, **50**, 2205–2207.
169 S. Manzini, D. J. Nelson, A. Poater, L. Cavallo, A. M. Z. Slawin and S. P. Nolan, *Angew. Chem., Int. Ed.*, 2014, DOI: 10.1002/anie.201403770.
170 T. M. Trnka, J. P. Morgan, M. S. Sanford, T. E. Wilhelm, M. Scholl, T.-L. Choi, S. Ding, M. W. Day and R. H. Grubbs, *J. Am. Chem. Soc.*, 2003, **125**, 2546–2558.
171 W. J. van Rensburg, P. J. Steynberg, W. H. Meyer, M. M. Kirk and G. S. Forman, *J. Am. Chem. Soc.*, 2004, **126**, 14332–14333.
172 W. J. van Rensburg, P. J. Steynberg, M. M. Kirk, W. H. Meyer and G. S. Forman, *J. Organomet. Chem.*, 2006, **691**, 5312–5325.